Modeling of photon scanning tunneling microscopy by 2-D quadridirectional eigenmode expansion

Manfred Hammer*

MESA$^+$ Research Institute
University of Twente, The Netherlands

PIERS 2004, Progress in Electromagnetics Research Symposium, Pisa, Italy, 28. – 31.03.2004

* *Department of Applied Mathematics, University of Twente* *P.O. Box 217, 7500 AE Enschede, The Netherlands*
Phone: +31/53/489-3448 *Fax: +31/53/489-4833* *E-mail: m.hammer@math.utwente.nl*

Photon scanning tunneling microscopy (PSTM) of photonic devices

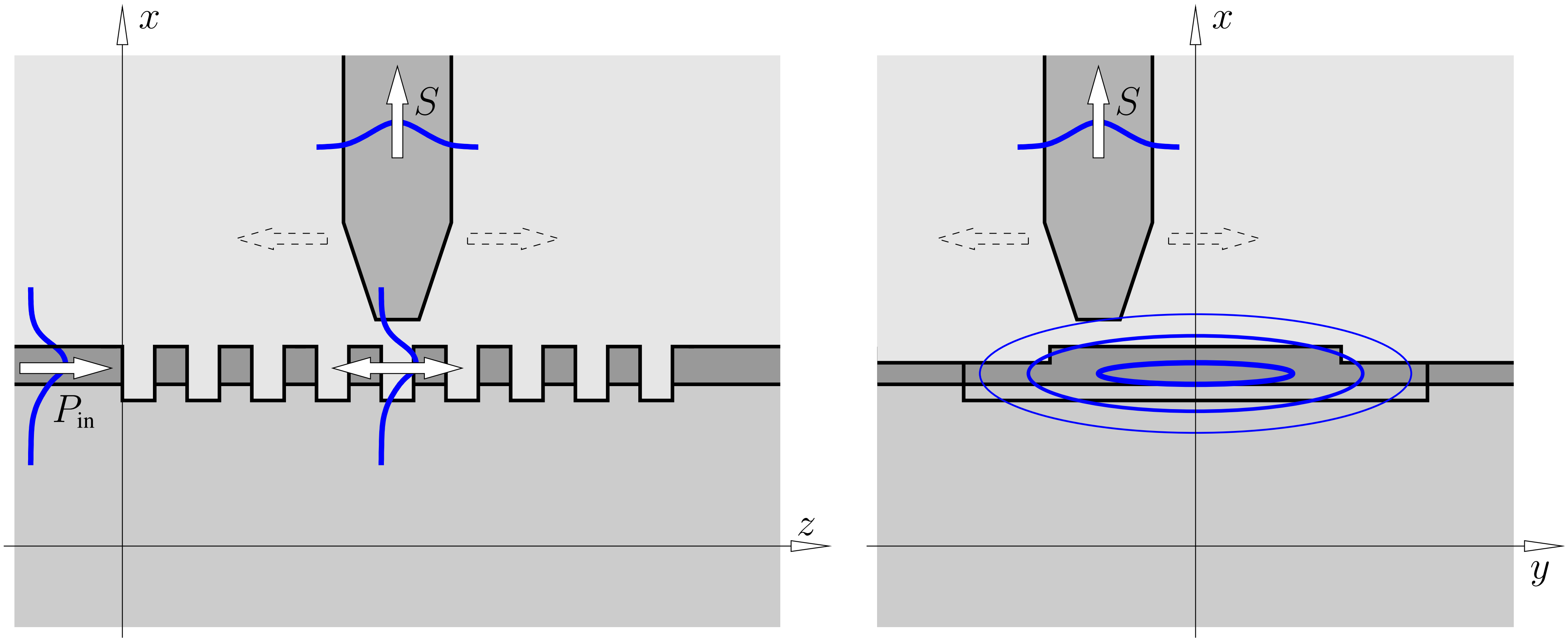

Simplified 2-D model

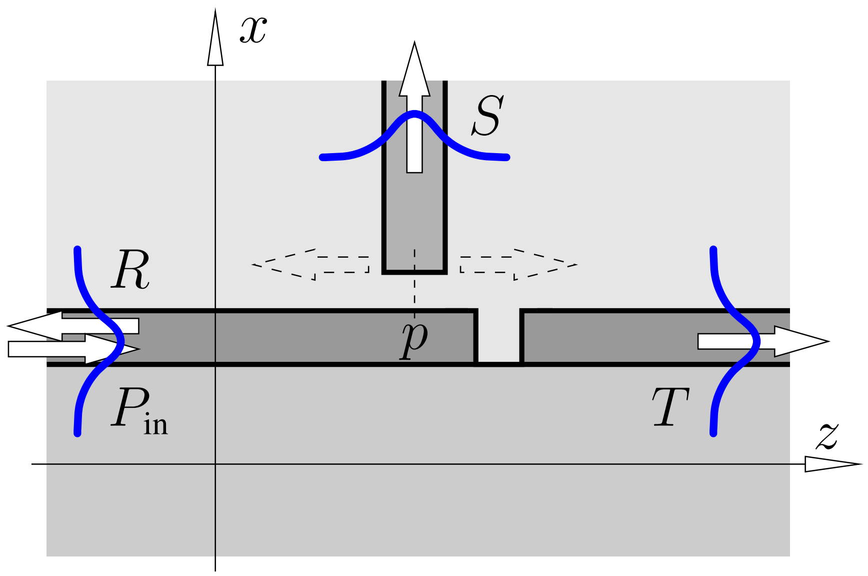

Simplified 2-D model

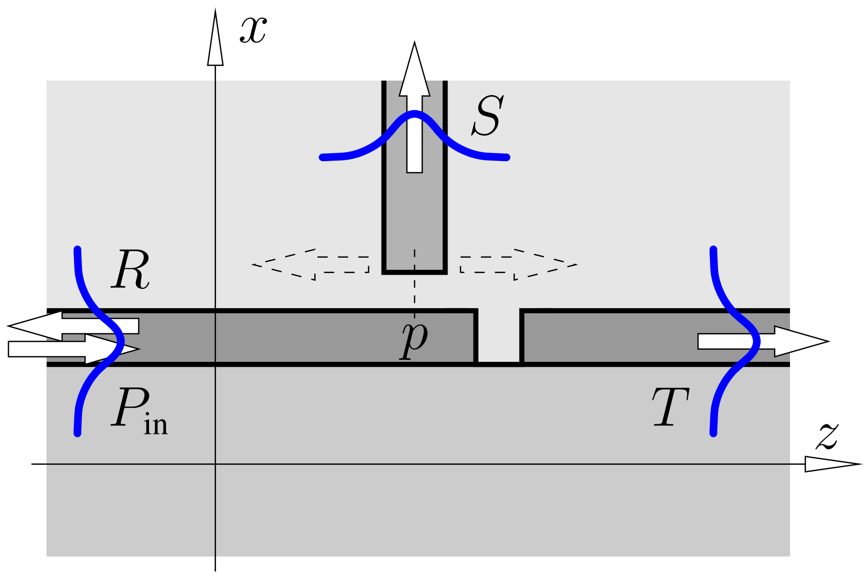

$$P_{\text{in}} = 1. \quad S(p) = ?$$

$$R(p),\, T(p) = ?$$

$$S(p) \overset{?}{\longleftrightarrow} (\text{optical field})\big|_p$$

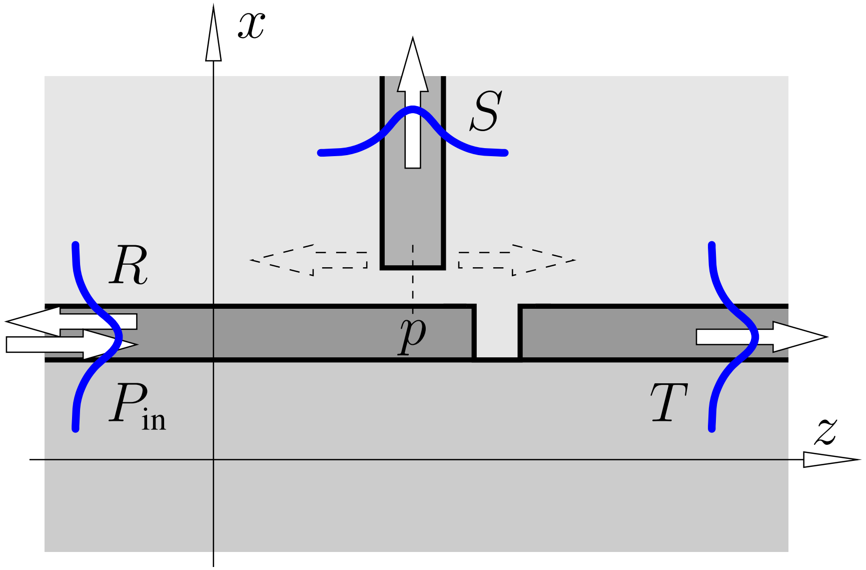

$$P_{\text{in}} = 1. \quad S(p) = ?$$

$$R(p),\, T(p) = ?$$

$$S(p) \stackrel{?}{\longleftrightarrow} (\text{optical field})\big|_p$$

Fixed optical frequency, rectangular piecewise constant refractive index, horizontal & vertical guided wave in- and outflux

$\longrightarrow$ *QUEP simulations*

Outline

- Quadridirectional eigenmode propagation:
    - Problem setting
    - Eigenmode expansion
    - Algebraic procedure

- 2-D PSTM model, numerical results:
    - Probing evanescent fields
    - Hole defect in a slab waveguide
    - Short waveguide Bragg grating
    - Resonant defect cavity
    - Bragg grating: PSTM experiment & 2-D model

Simulations, problem setting

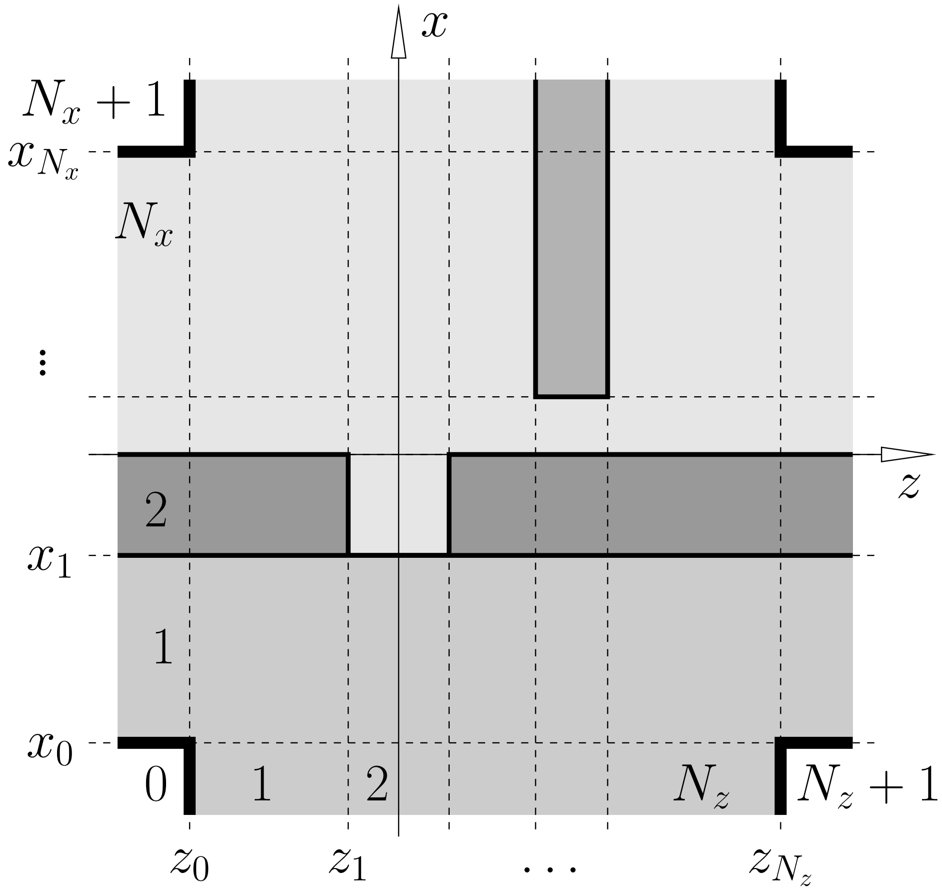

- 2-D TE/TM Helmholtz problem, vacuum wavelength $\lambda = 2\pi/k$.

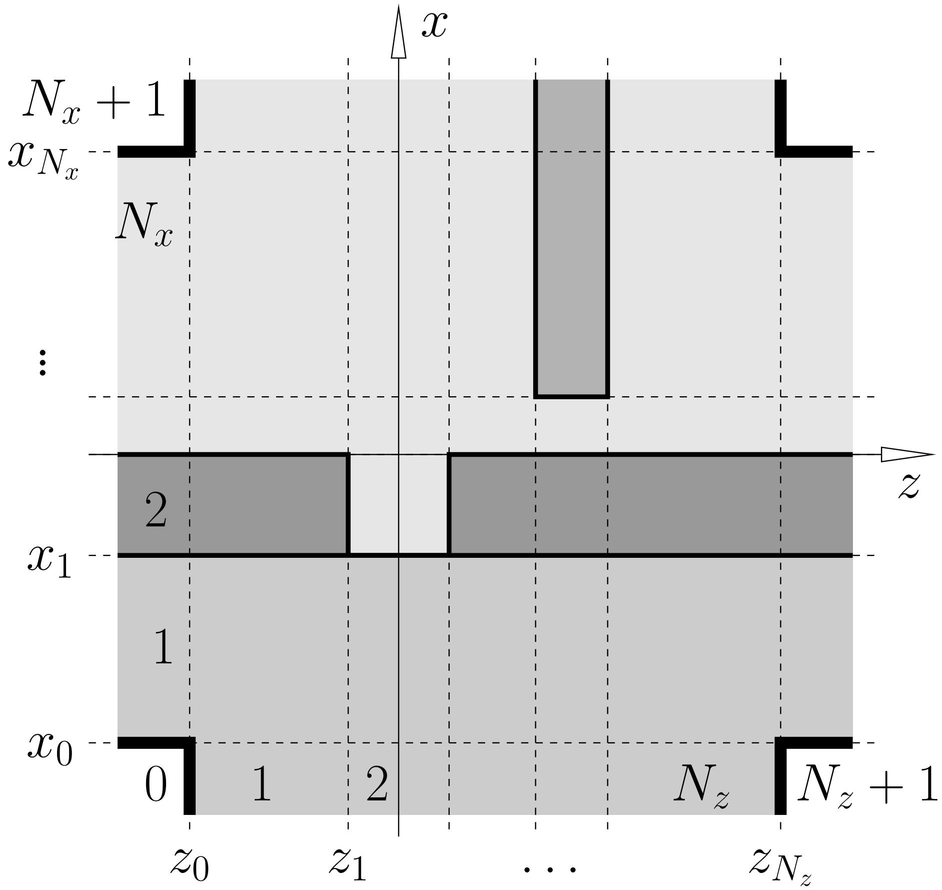

- 2-D TE/TM Helmholtz problem, vacuum wavelength $\lambda = 2\pi/k$.
- Piecewise constant, rectangular refractive index distribution; linear, lossless materials.

Simulations, problem setting

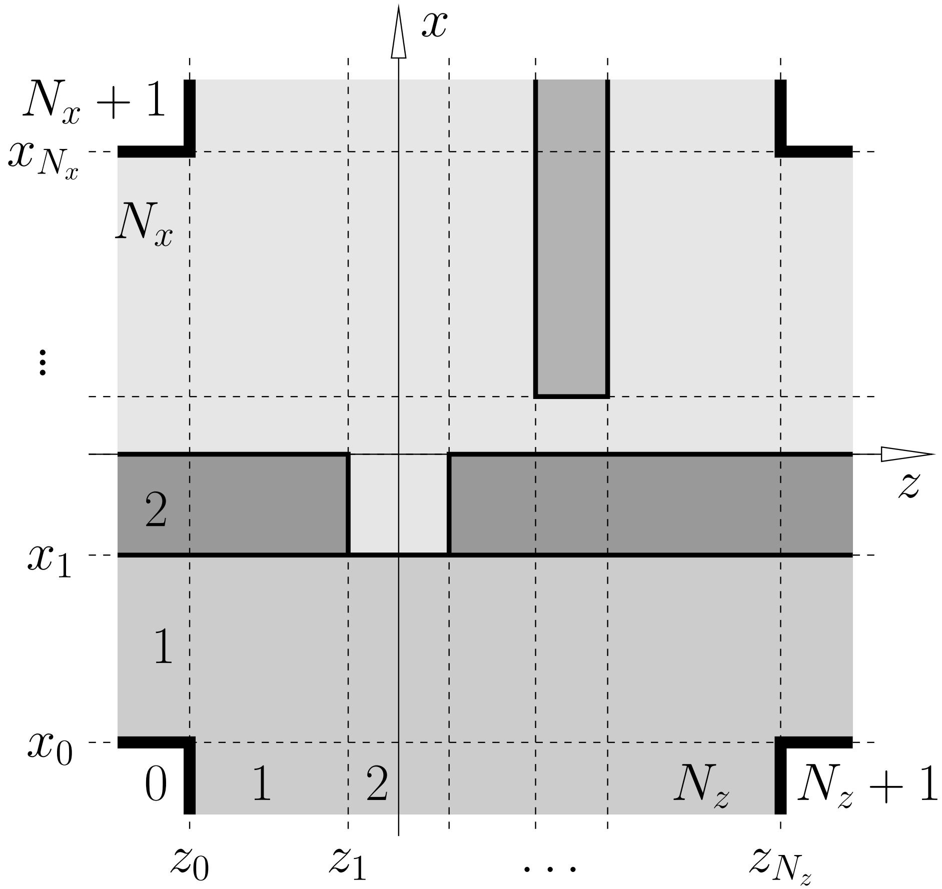

- 2-D TE/TM Helmholtz problem, vacuum wavelength $\lambda = 2\pi/k$.
- Piecewise constant, rectangular refractive index distribution; linear, lossless materials.
- Rectangular interior computational domain, influx & outflux across all four boundaries, outwards homogeneous external regions.

Simulations, problem setting

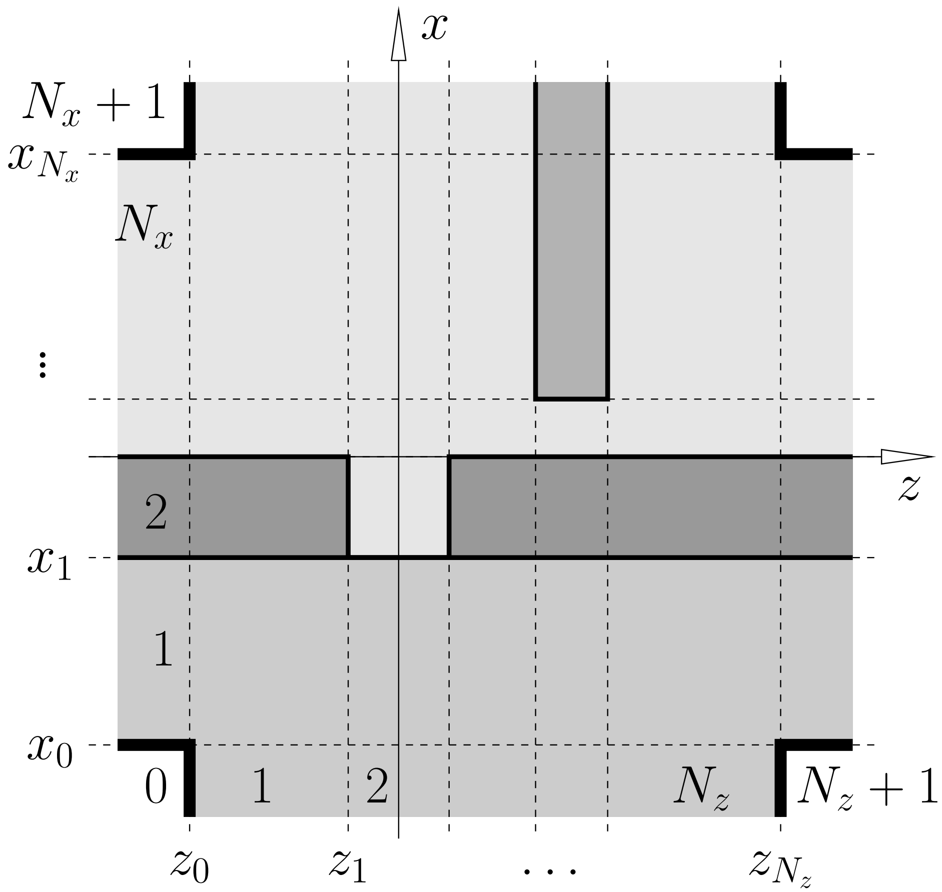

- 2-D TE/TM Helmholtz problem, vacuum wavelength $\lambda = 2\pi/k$.
- Piecewise constant, rectangular refractive index distribution; linear, lossless materials.
- Rectangular interior computational domain, influx & outflux across all four boundaries, outwards homogeneous external regions.
- Assumption $E_y = 0$, $H_y = 0$ on the corner points and on the external border lines is reasonable for the problems under investigation.

Modal basis fields

Basis fields,
defined by Dirichlet boundary conditions $E_y = 0$ (TE) or $H_y = 0$ (TM):

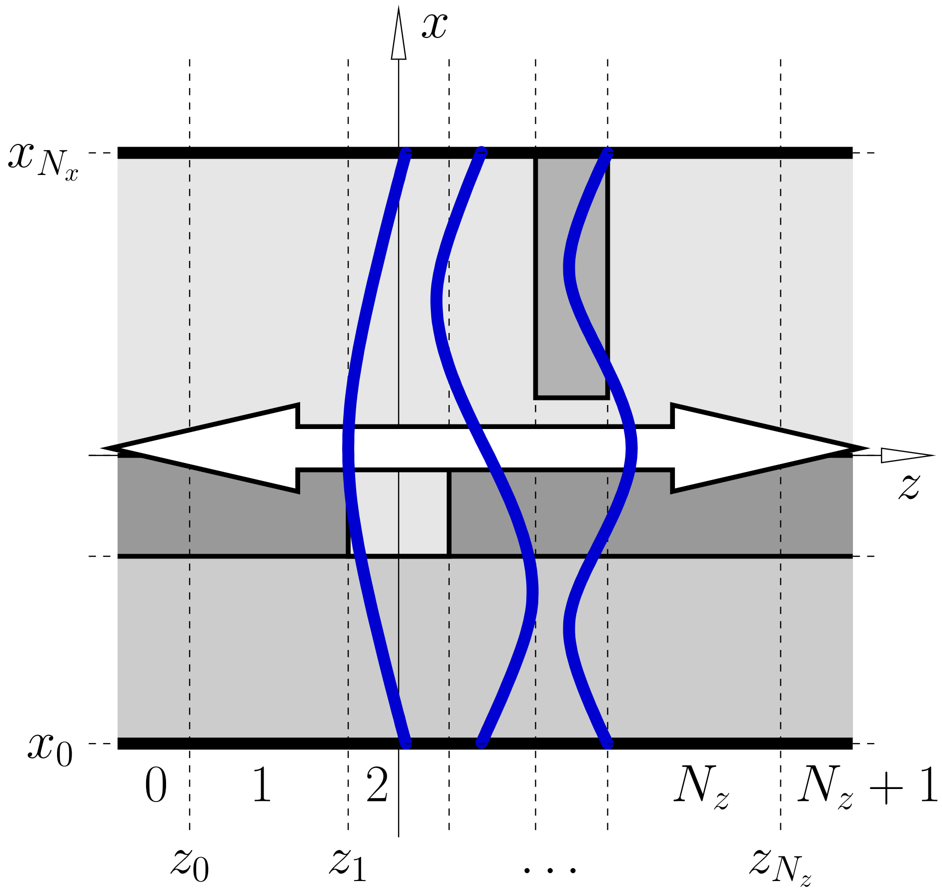

Horizontally traveling eigenmodes:

M_x profiles	$\boldsymbol{\psi}^d_{s,m}(x)$
and propagation constants	$\pm\beta_{s,m}$

of order m, on slice s,
for propagation directions $d = \mathrm{f}, \mathrm{b}$,

Modal basis fields

Basis fields,
defined by Dirichlet boundary conditions $E_y = 0$ (TE) or $H_y = 0$ (TM):

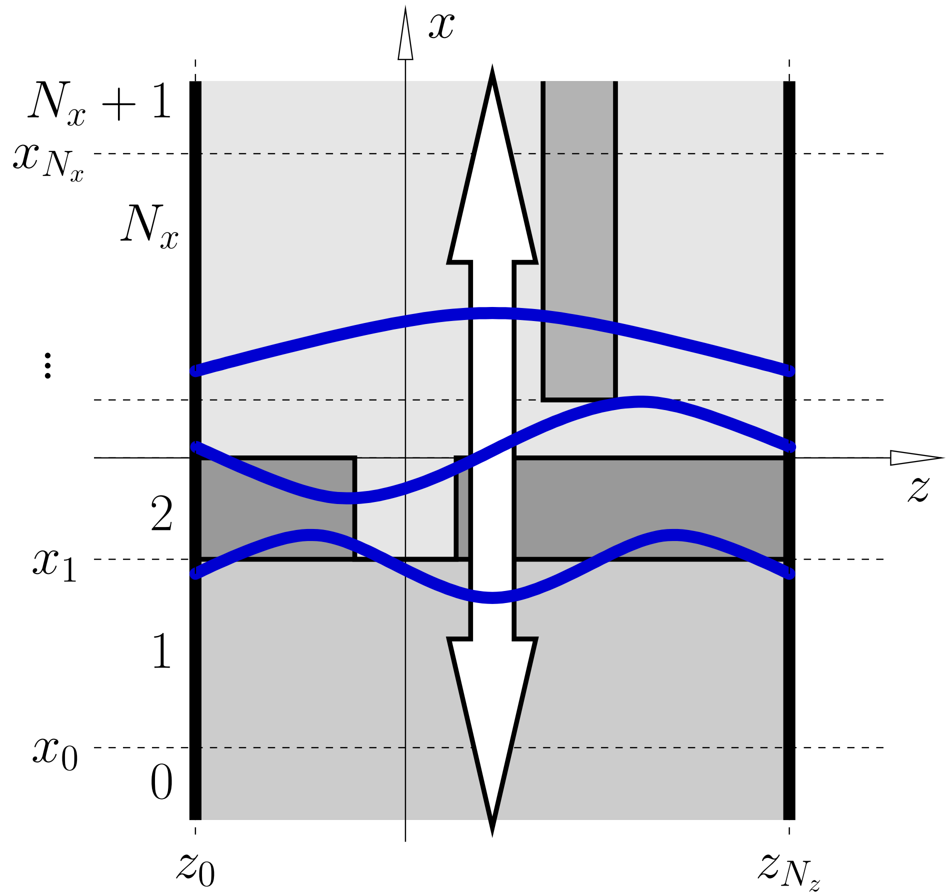

… *and* vertically traveling fields:

M_z profiles	$\hat{\boldsymbol{\psi}}^d_{l,m}(z)$
and propagation constants	$\pm\hat{\beta}_{l,m}$

of order m, on layer l,
for propagation directions $d =$ u, d.

Eigenmode expansion

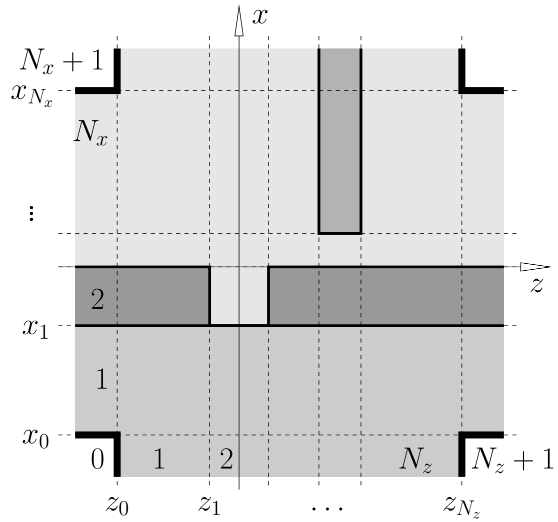

Ansatz for the optical field,
for $z_{s-1} \le z \le z_s,\ s = 1, \dots, N_z$,
and $x_{l-1} \le x \le x_l$, $l = 1, \dots, N_x$:

$$\begin{pmatrix} \boldsymbol{\mathcal{E}} \\ \boldsymbol{\mathcal{H}} \end{pmatrix}(x, z, t) = \mathrm{Re}\left\{ \sum_{m=0}^{M_x - 1} F_{s,m} \boldsymbol{\psi}^{\mathrm{f}}_{s,m}(x)\, \mathrm{e}^{-\mathrm{i}\beta_{s,m}(z - z_{s-1})} \right.$$

$$+ \sum_{m=0}^{M_x - 1} B_{s,m} \boldsymbol{\psi}^{\mathrm{b}}_{s,m}(x)\, \mathrm{e}^{+\mathrm{i}\beta_{s,m}(z - z_s)}$$

$$+ \sum_{m=0}^{M_z - 1} U_{l,m} \hat{\boldsymbol{\psi}}^{\mathrm{u}}_{l,m}(z)\, \mathrm{e}^{-\mathrm{i}\hat{\beta}_{l,m}(x - x_{l-1})}$$

$$\left. + \sum_{m=0}^{M_z - 1} D_{l,m} \hat{\boldsymbol{\psi}}^{\mathrm{d}}_{l,m}(z)\, \mathrm{e}^{+\mathrm{i}\hat{\beta}_{l,m}(x - x_l)} \right\} \mathrm{e}^{\mathrm{i}\omega t}.$$

Eigenmode expansion

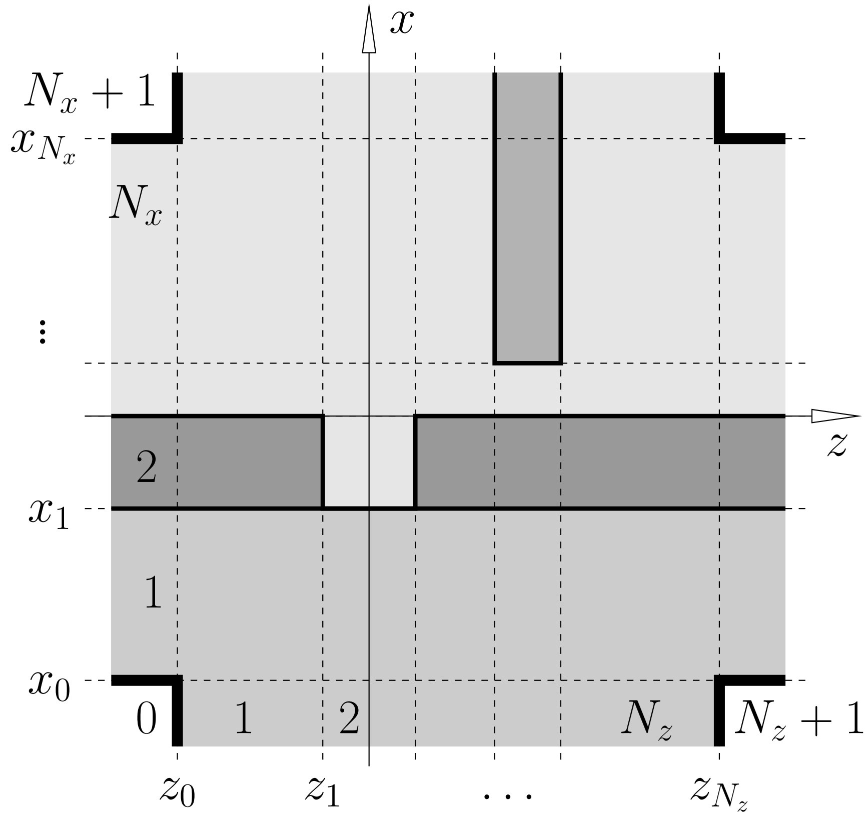

Mode products ↔ normalization, projection:

$$(\boldsymbol{E}_1, \boldsymbol{H}_1; \boldsymbol{E}_2, \boldsymbol{H}_2) = \frac{1}{4} \int (E^*_{1,x} H_{2,y} - E^*_{1,y} H_{2,x} + H^*_{1,y} E_{2,x} - H^*_{1,x} E_{2,y})\, \mathrm{d}x \,,$$

$$\langle \boldsymbol{E}_1, \boldsymbol{H}_1; \boldsymbol{E}_2, \boldsymbol{H}_2 \rangle = \frac{1}{4} \int (E^*_{1,y} H_{2,z} - E^*_{1,z} H_{2,y} + H^*_{1,z} E_{2,y} - H^*_{1,y} E_{2,z})\, \mathrm{d}z \,.$$

Algebraic procedure

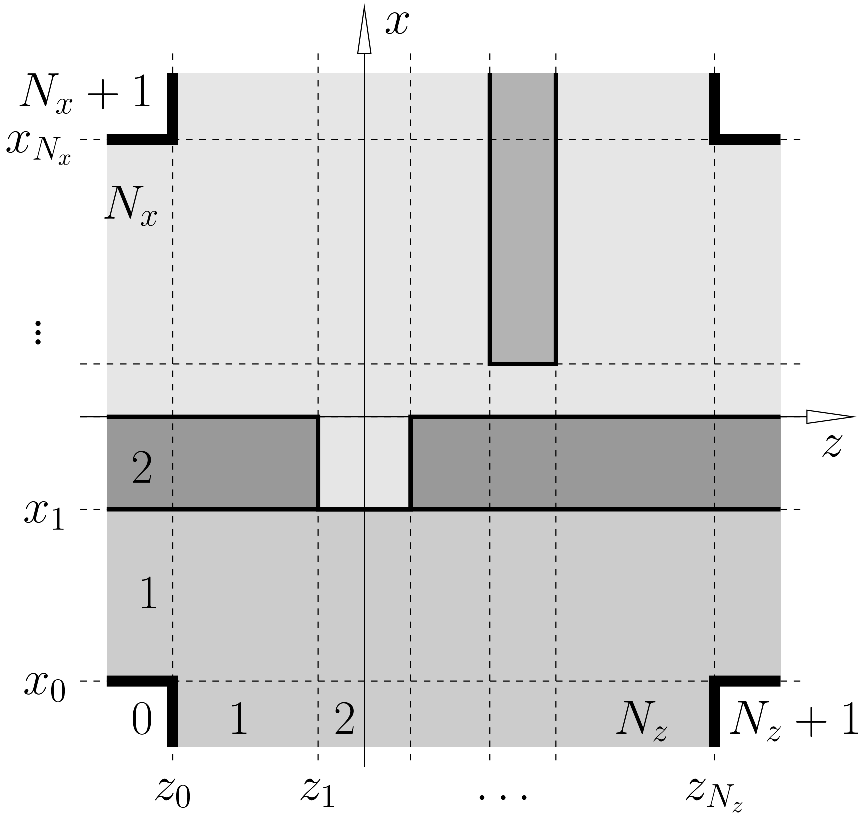

- Consistent bidirectional projection at all interfaces
  $\longrightarrow$ linear system of equations in $\{F_{s,m}, B_{s,m}, U_{l,m}, D_{l,m}\}$.
- Influx: $\boldsymbol{F}_0,\ \boldsymbol{B}_{N_x+1},\ \boldsymbol{U}_0,\ \boldsymbol{D}_{N_z+1} \longrightarrow$ RHS, given.
- Outflux: $\boldsymbol{B}_0,\ \boldsymbol{F}_{N_x+1},\ \boldsymbol{D}_0,\ \boldsymbol{U}_{N_z+1} \longrightarrow$ primary unknowns.

Algebraic procedure

- "Exact" mode profiles $\longrightarrow$ interior problems decouple:

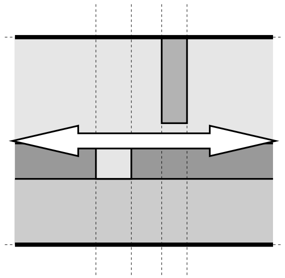

Solve for $\boldsymbol{F}_2, \ldots, \boldsymbol{F}_{N_z}$ and $\boldsymbol{B}_1, \ldots, \boldsymbol{B}_{N_z-1}$ in terms of $\boldsymbol{F}_1$ and $\boldsymbol{B}_{N_z}$ $\longrightarrow$ BEP I.

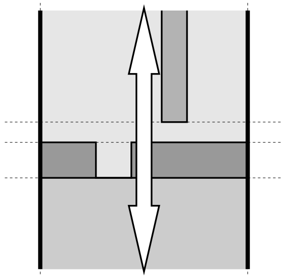

Solve for $\boldsymbol{U}_2, \ldots, \boldsymbol{U}_{N_x}$ and $\boldsymbol{D}_1, \ldots, \boldsymbol{D}_{N_x-1}$ in terms of $\boldsymbol{U}_1$ and $\boldsymbol{D}_{N_x}$ $\longrightarrow$ BEP II.

- Continuity of E and H on outer interfaces:

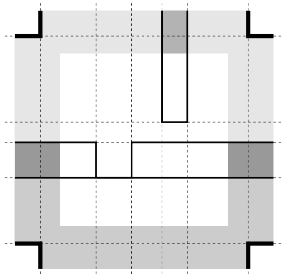

Interior BEP solutions
$+$ equations at $z = z_0, z_{N_z},\ x = x_0, x_{N_x}$
$\longrightarrow \boldsymbol{B}_0,\ \boldsymbol{F}_{N_x+1},\ \boldsymbol{D}_0,\ \boldsymbol{U}_{N_z+1}$.

"QUadridirectional Eigenmode Propagation method" (QUEP).

Probing evanescent fields

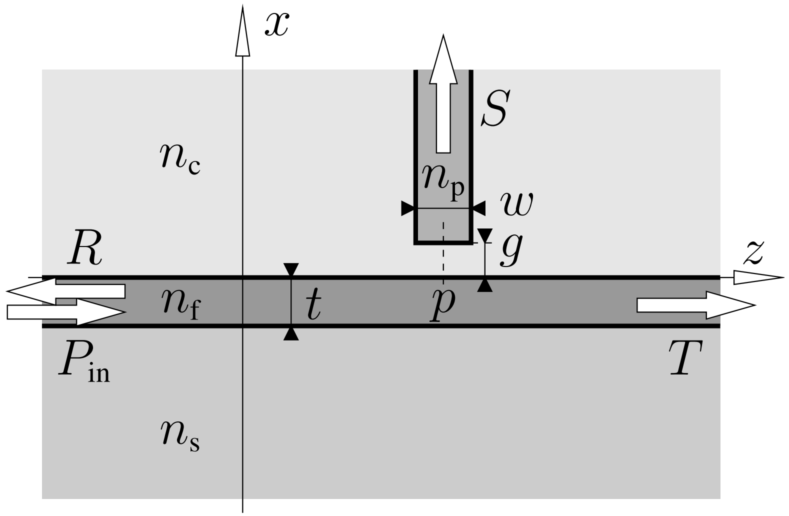

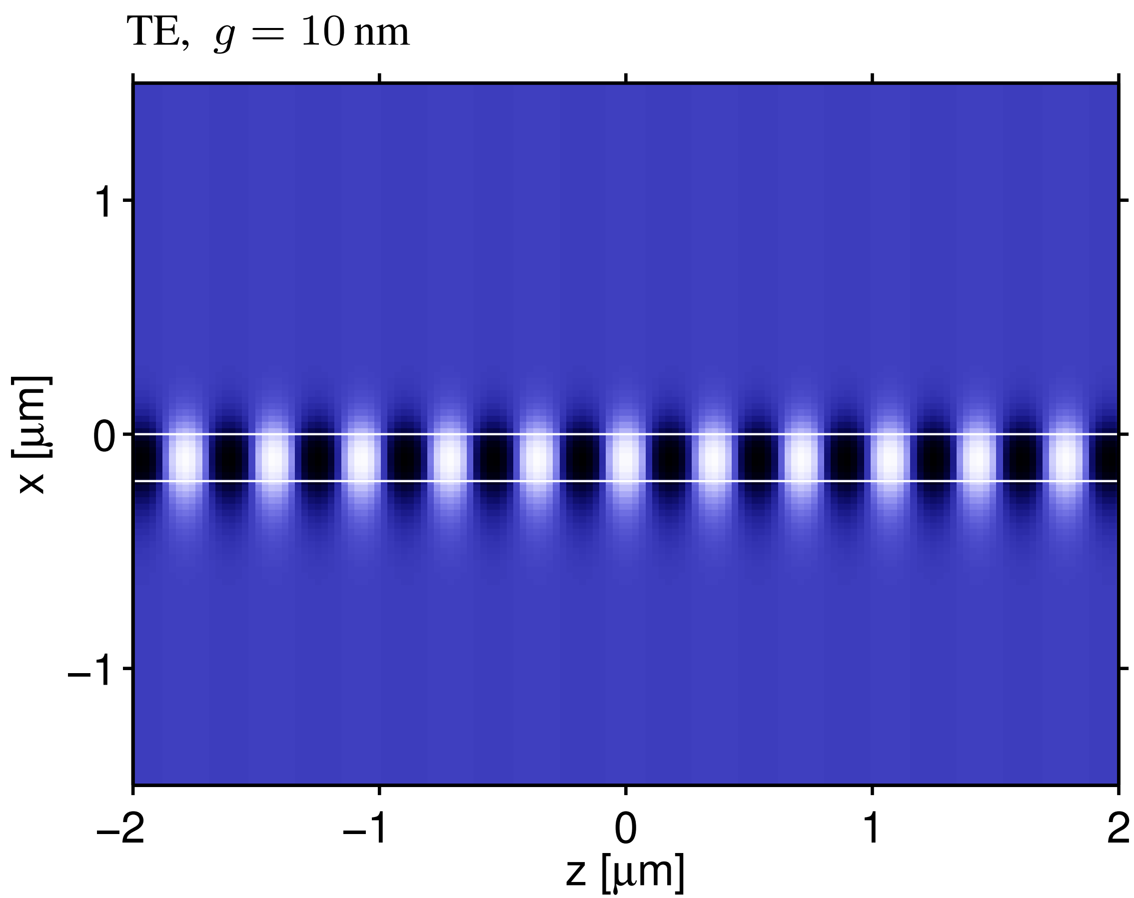

$n_s = 1.45$, $n_f = 2.0$, $n_c = 1.0$, $t = 0.2\,\mu$m, $w = 100\,$nm, $n_p = 1.5$,
$\lambda = 0.633\,\mu$m, $(x, z) \in [-3.0, 3.0] \times [-3.0, 3.0]\,\mu\text{m}^2$, $M_x = M_z = 80$.

Probing evanescent fields

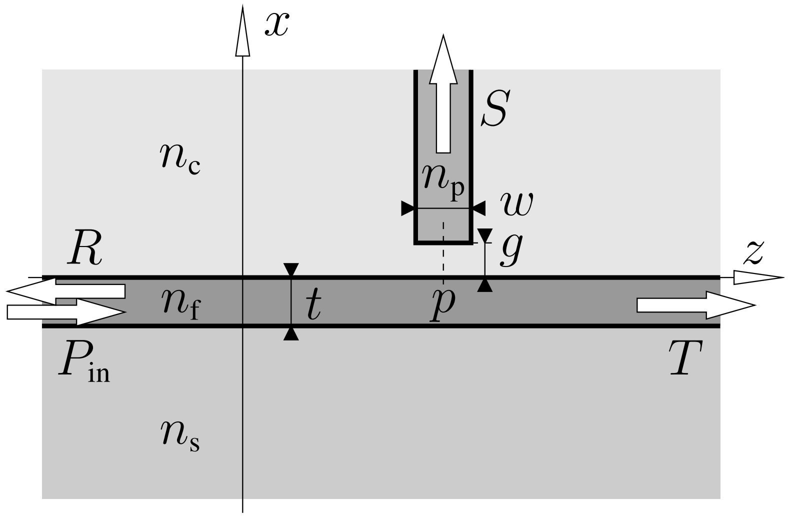

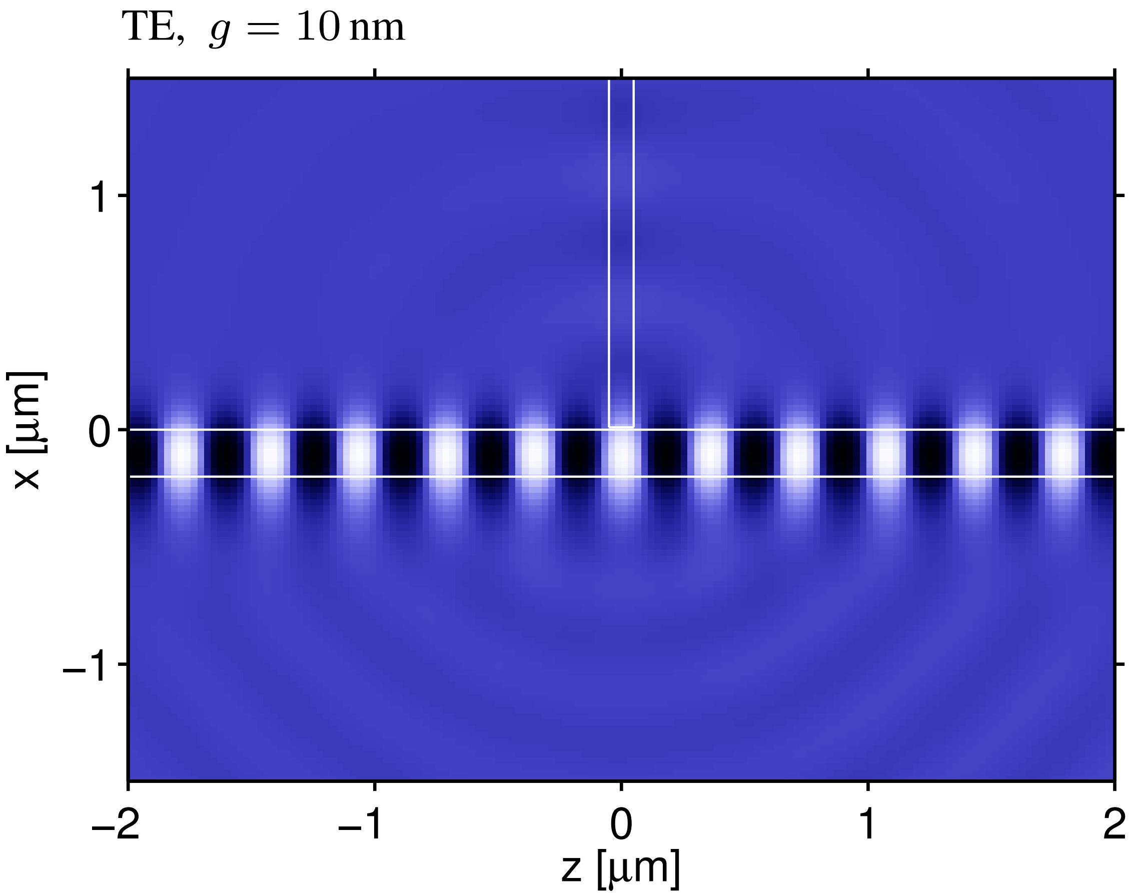

$n_s = 1.45$, $n_f = 2.0$, $n_c = 1.0$, $t = 0.2\,\mu$m, $w = 100\,$nm, $n_p = 1.5$,
$\lambda = 0.633\,\mu$m, $(x, z) \in [-3.0, 3.0] \times [-3.0, 3.0]\,\mu\text{m}^2$, $M_x = M_z = 80$.

Probing evanescent fields

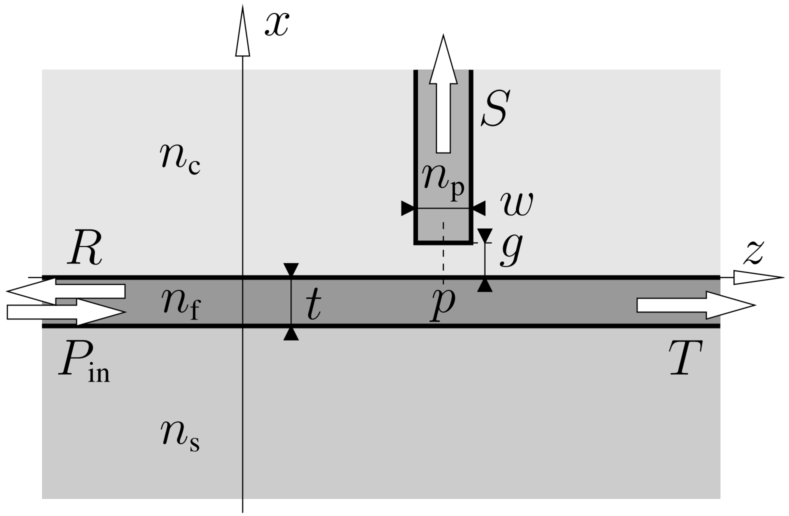

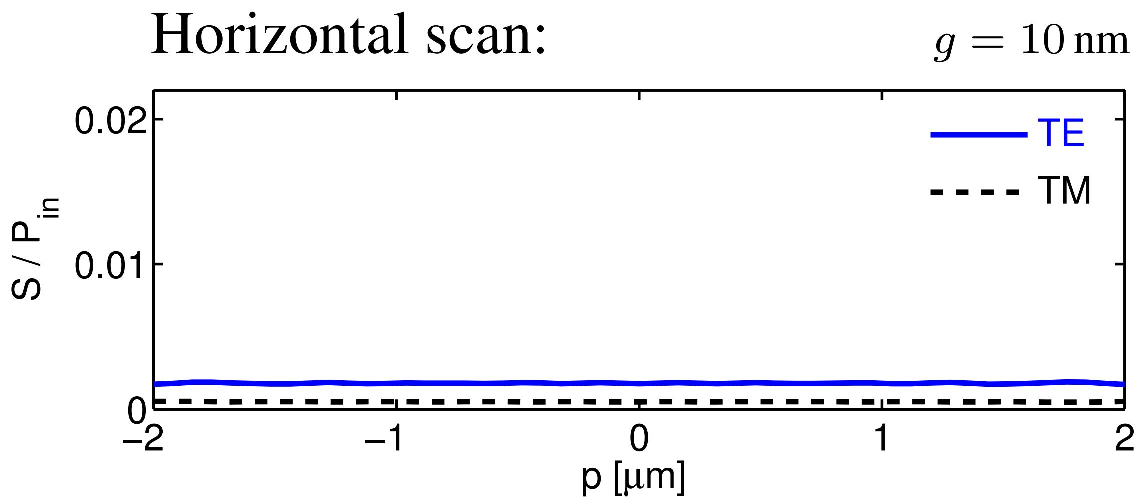

$n_s = 1.45$, $n_f = 2.0$, $n_c = 1.0$, $t = 0.2\,\mu$m, $w = 100\,$nm, $n_p = 1.5$,
$\lambda = 0.633\,\mu$m, $(x, z) \in [-3.0, 3.0] \times [-3.0, 3.0]\,\mu\mathrm{m}^2$, $M_x = M_z = 80$.

Probing evanescent fields

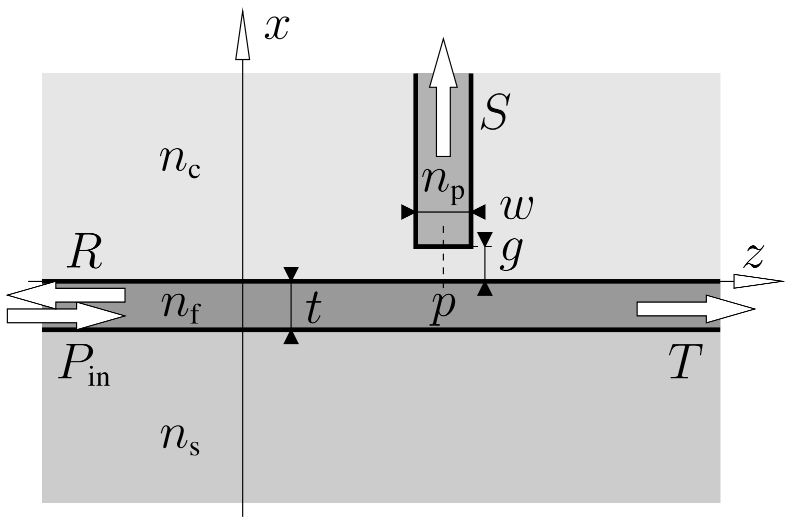

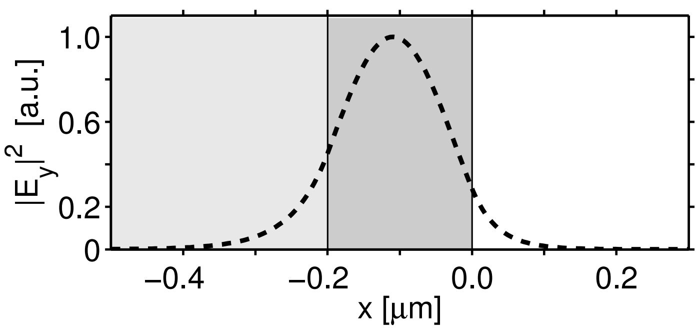

Vertical scan: TE

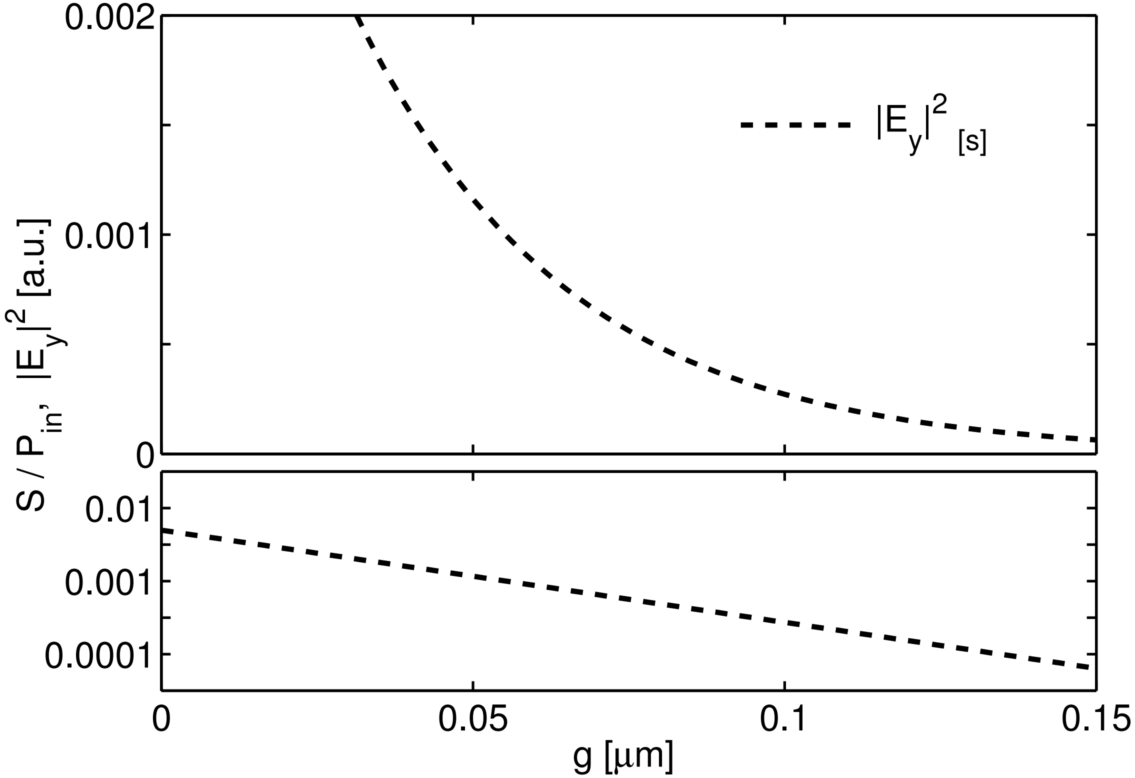

Probing evanescent fields

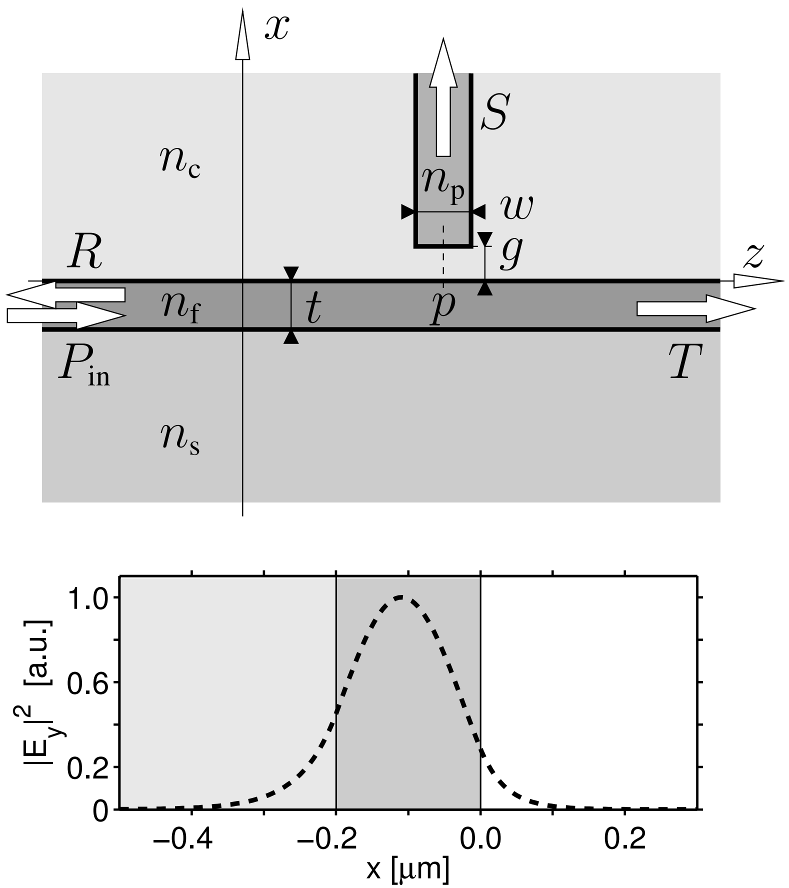

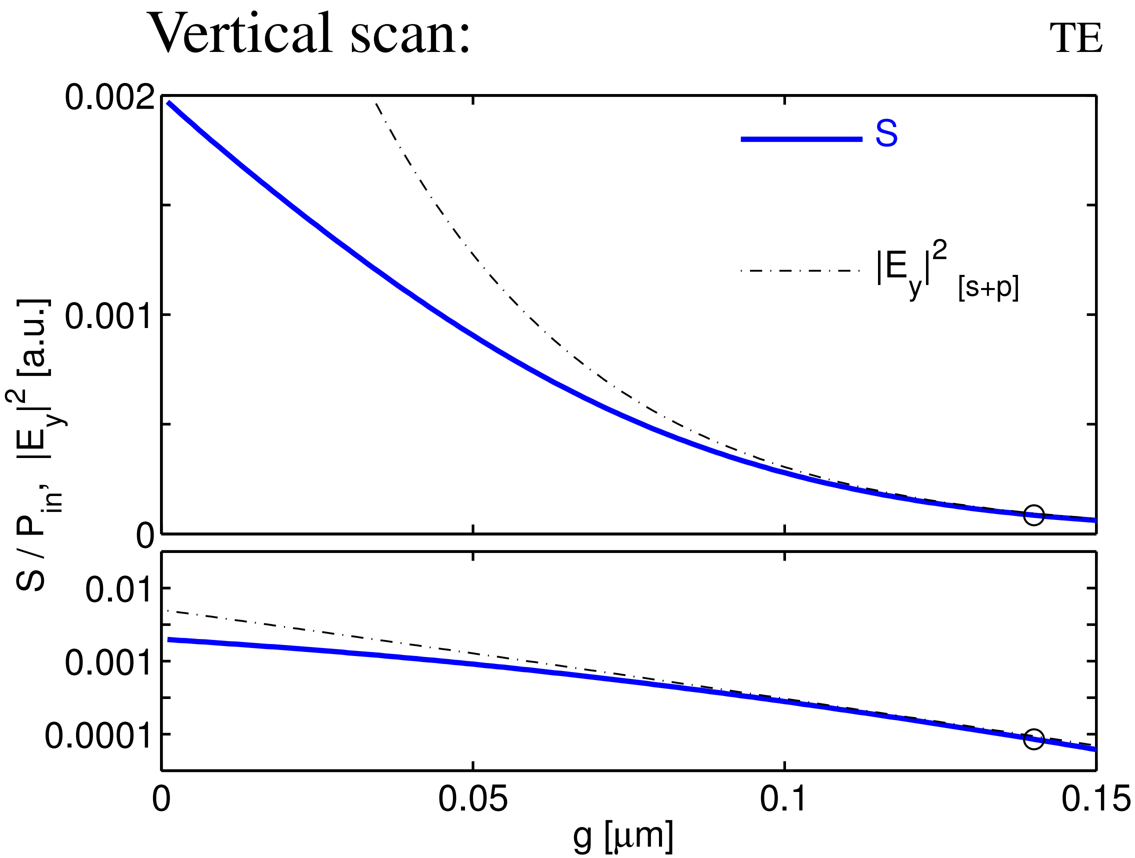

Probing evanescent fields

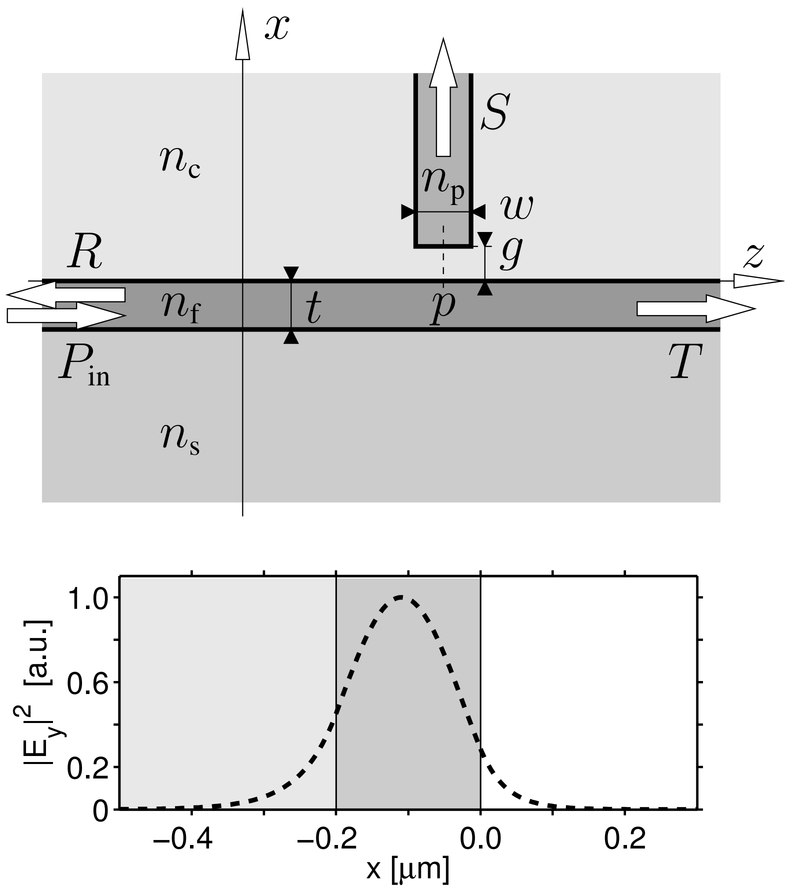

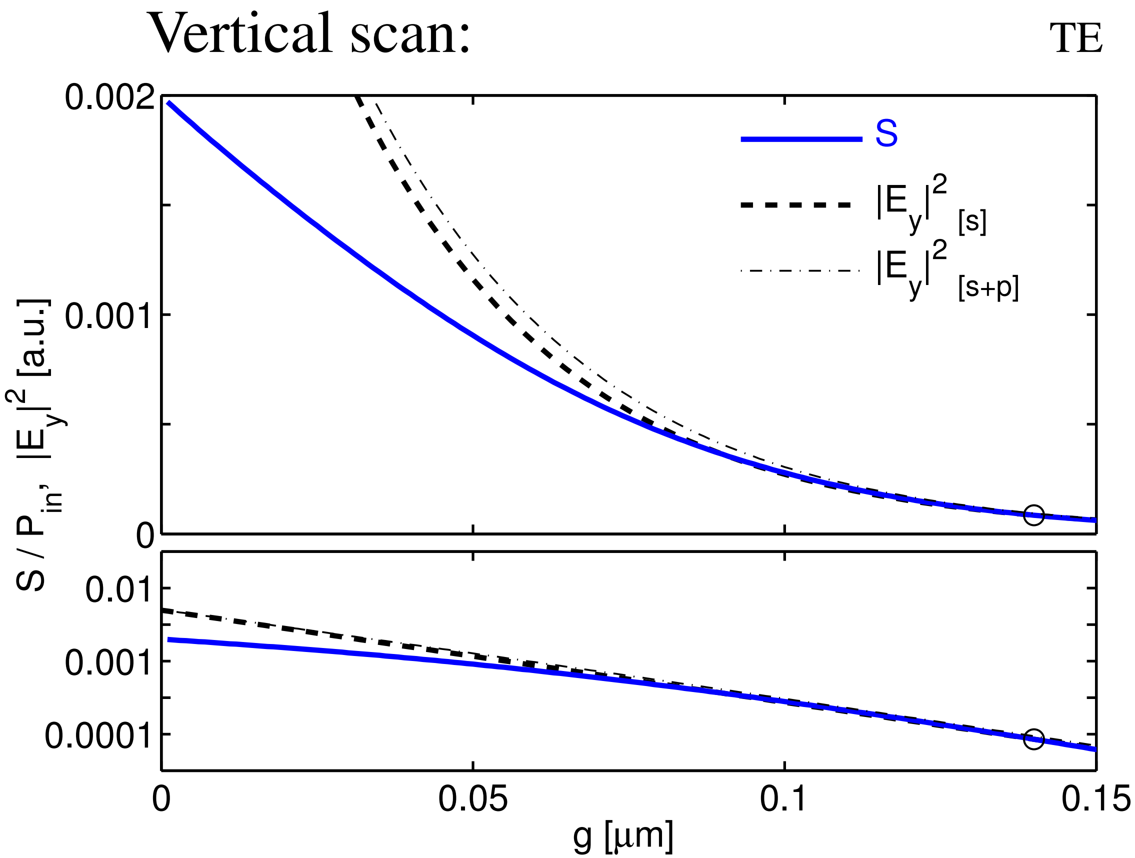

Probing evanescent fields

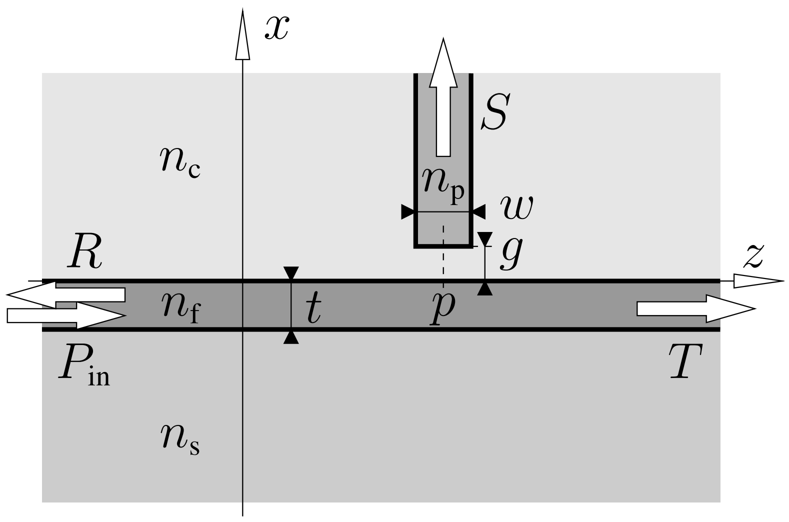

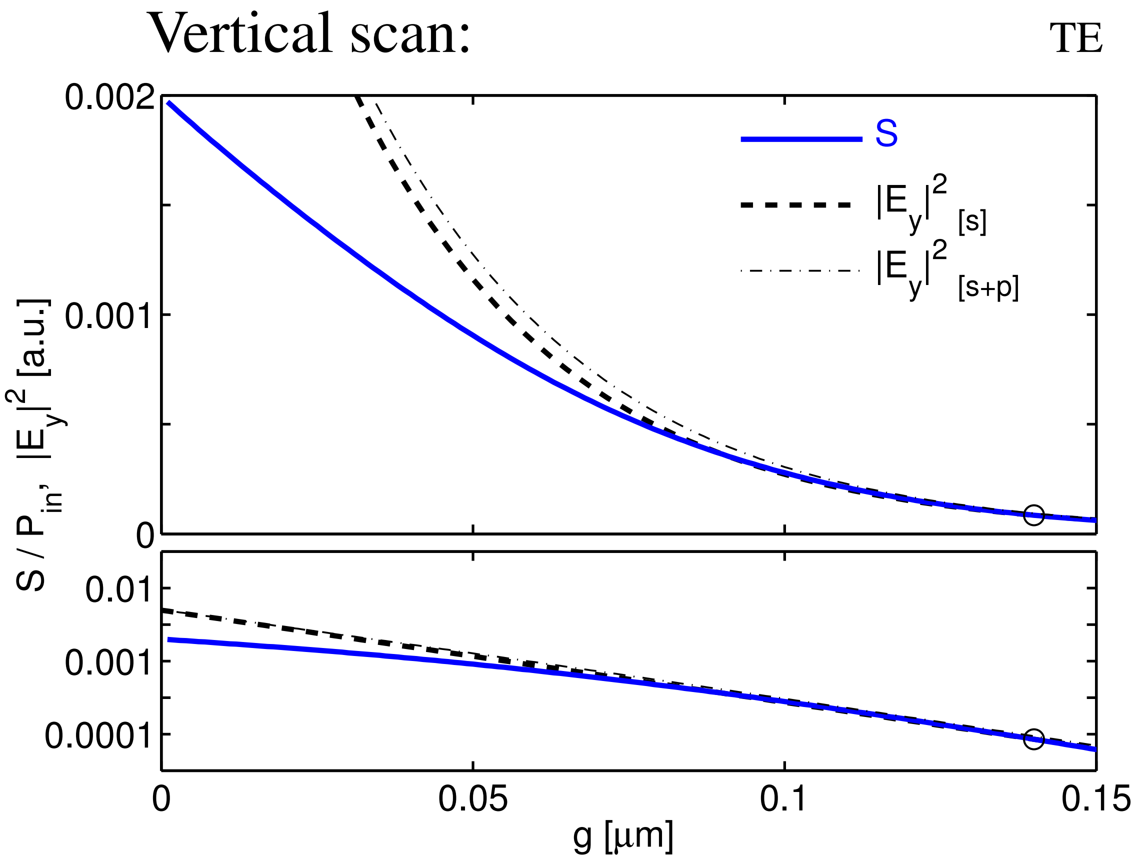

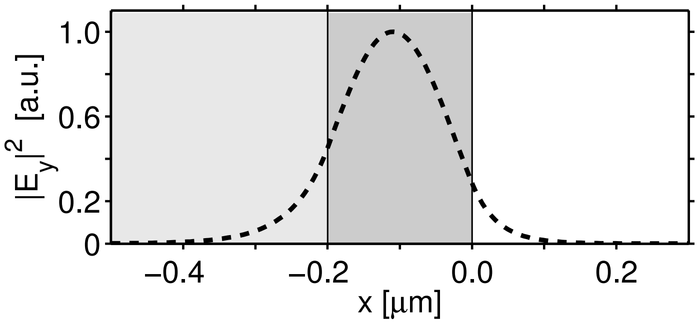

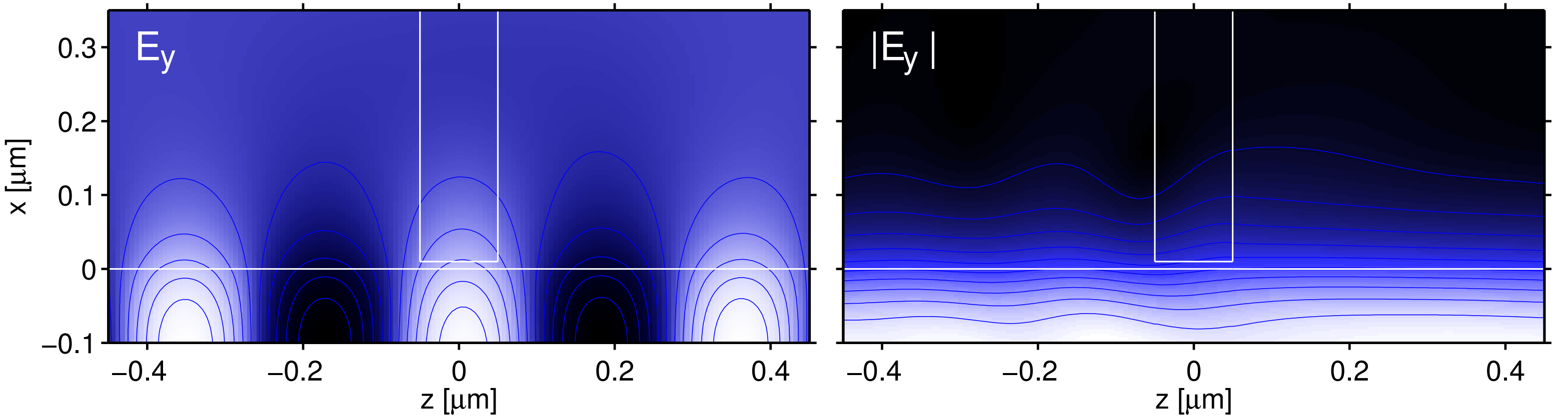

Hole defect in a slab waveguide

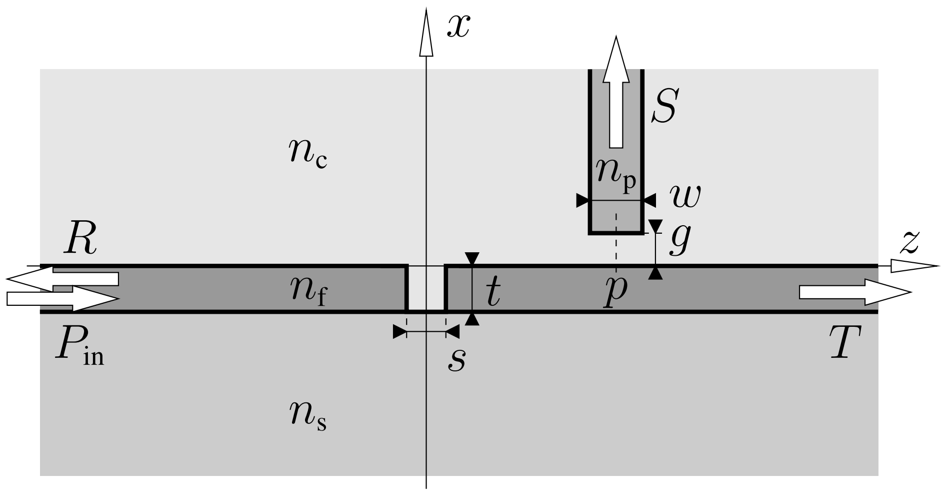

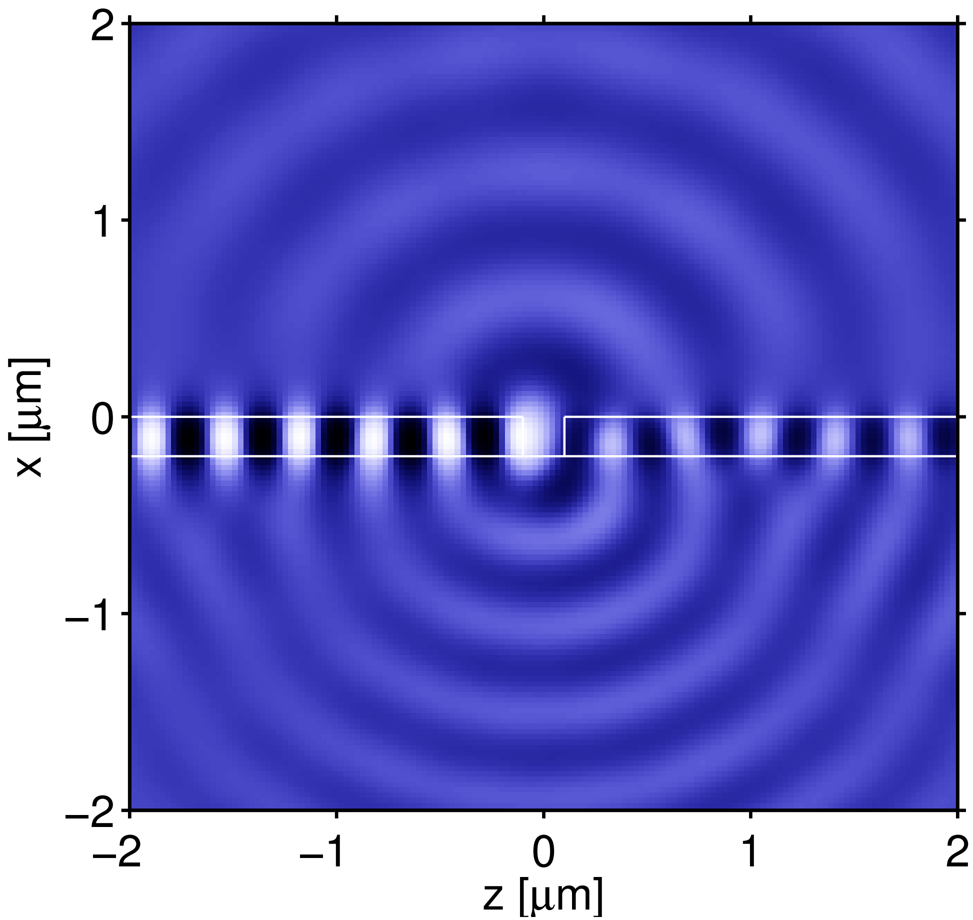

$n_s = 1.45$, $n_f = 2.0$, $n_c = 1.0$, $t = 0.2\,\mu$m, $s = 0.2\,\mu$m, $g = 10\,$nm, $w = 100\,$nm, $n_p = 1.5$,
TE, $\lambda = 0.633\,\mu$m, $(x, z) \in [-3.0, 3.0] \times [-3.1, 3.1]\,\mu\text{m}^2$, $M_x = M_z = 80$.

Hole defect in a slab waveguide

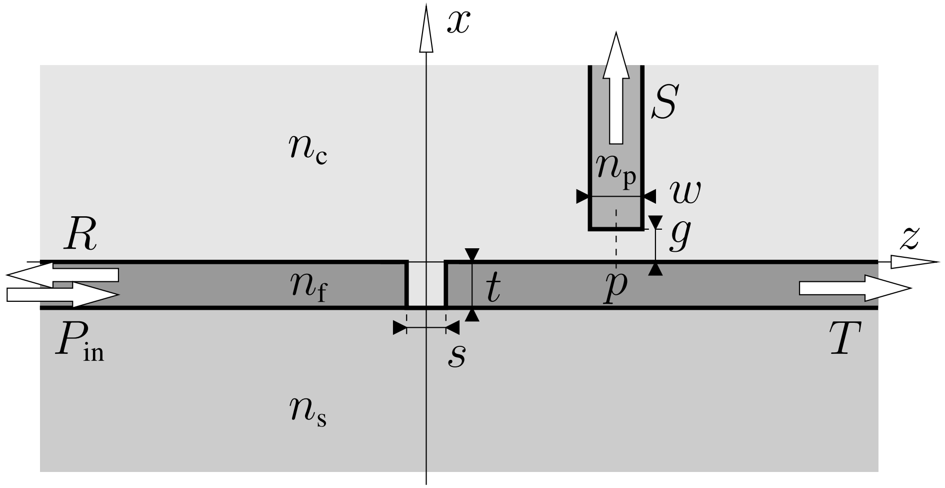

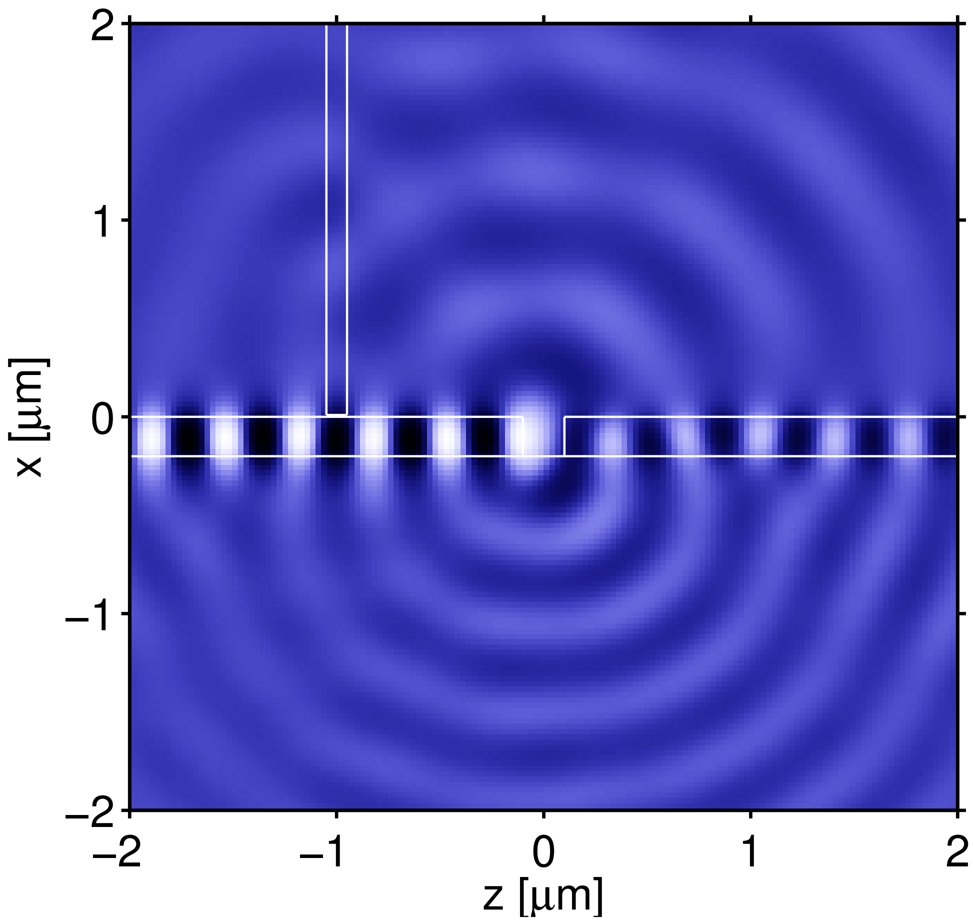

$n_s = 1.45$, $n_f = 2.0$, $n_c = 1.0$, $t = 0.2\,\mu$m, $s = 0.2\,\mu$m, $g = 10\,$nm, $w = 100\,$nm, $n_p = 1.5$,
TE, $\lambda = 0.633\,\mu$m, $(x, z) \in [-3.0, 3.0] \times [-3.1, 3.1]\,\mu\text{m}^2$, $M_x = M_z = 80$.

Hole defect in a slab waveguide

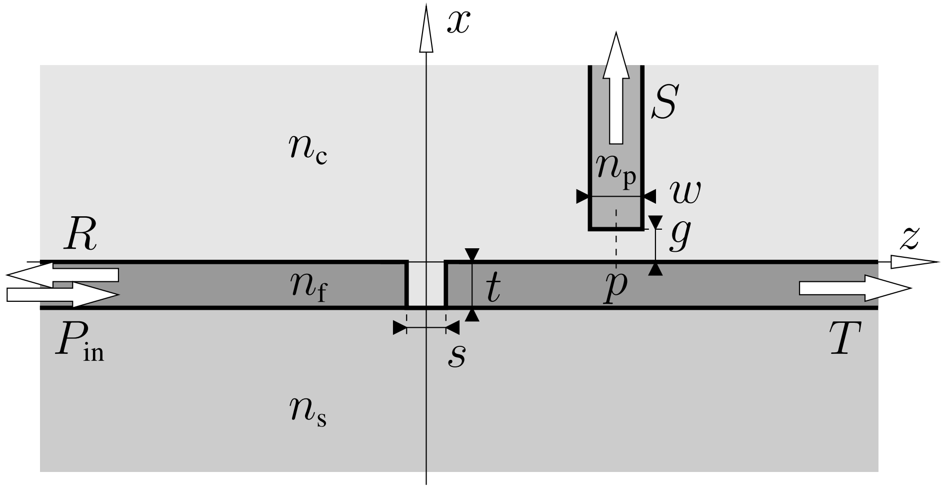

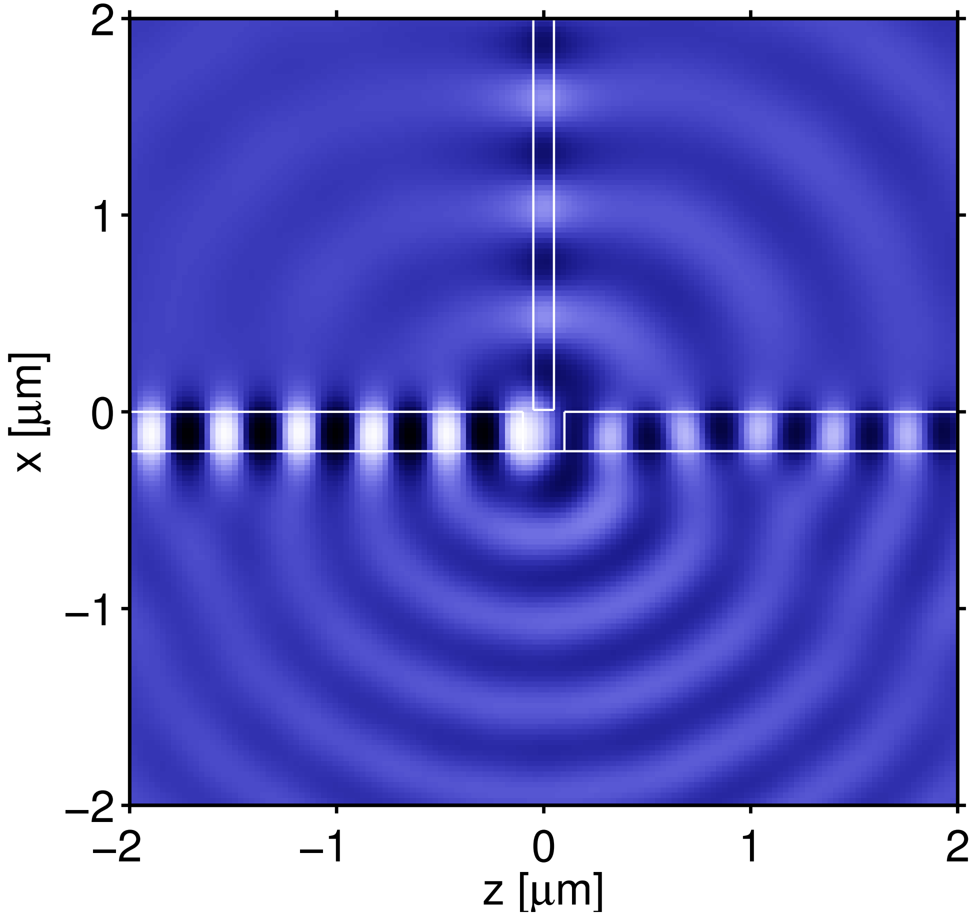

$n_s = 1.45$, $n_f = 2.0$, $n_c = 1.0$, $t = 0.2\,\mu$m, $s = 0.2\,\mu$m, $g = 10\,$nm, $w = 100\,$nm, $n_p = 1.5$,
TE, $\lambda = 0.633\,\mu$m, $(x, z) \in [-3.0, 3.0] \times [-3.1, 3.1]\,\mu\text{m}^2$, $M_x = M_z = 80$.

Hole defect in a slab waveguide

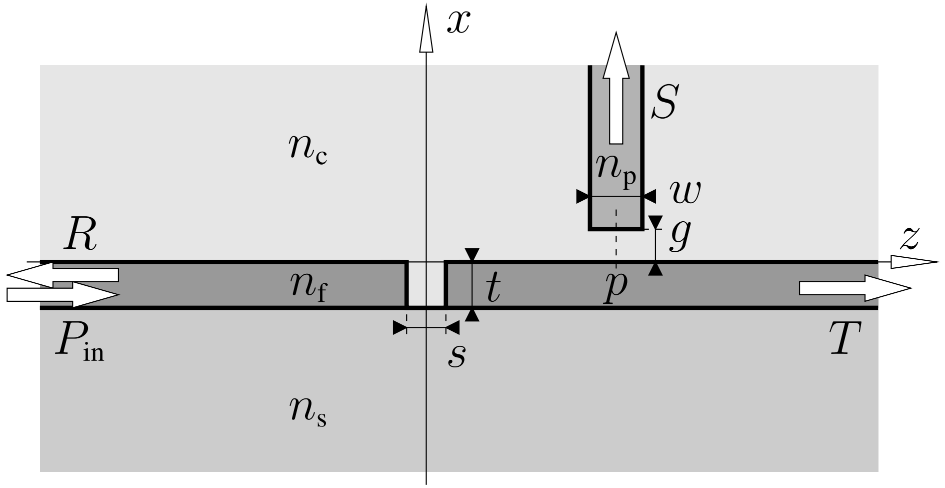

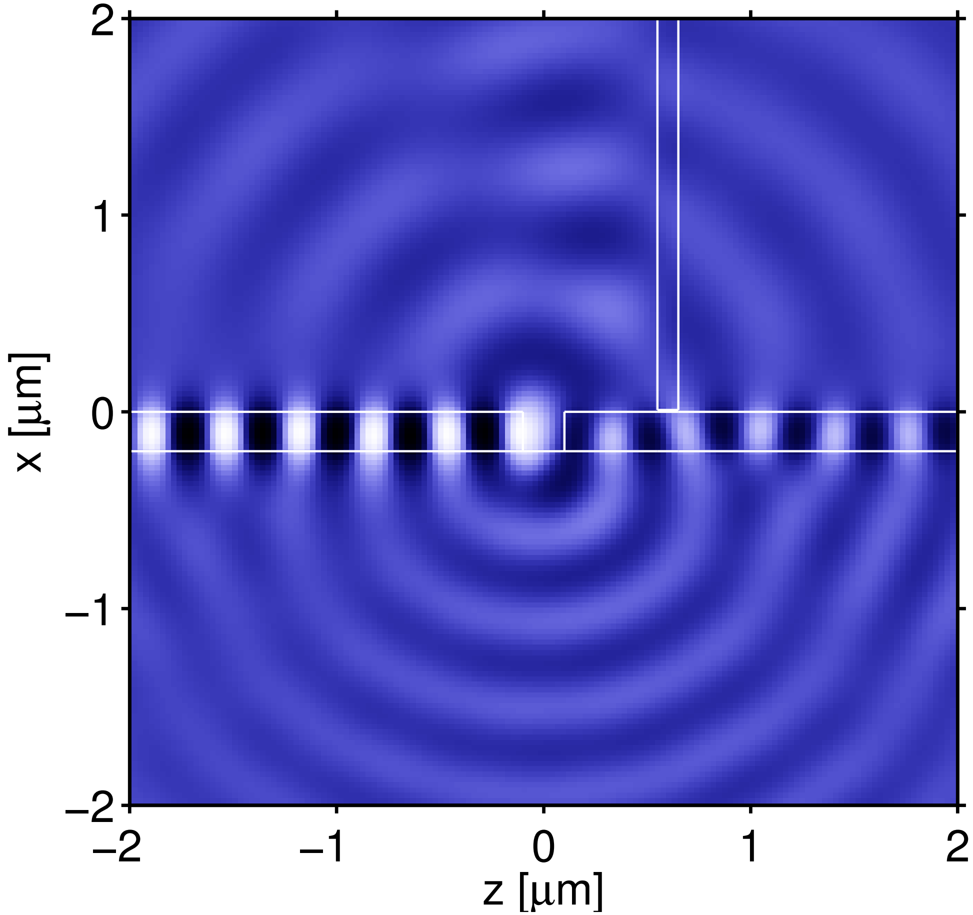

$n_s = 1.45$, $n_f = 2.0$, $n_c = 1.0$, $t = 0.2\,\mu$m, $s = 0.2\,\mu$m, $g = 10\,$nm, $w = 100\,$nm, $n_p = 1.5$,
TE, $\lambda = 0.633\,\mu$m, $(x, z) \in [-3.0, 3.0] \times [-3.1, 3.1]\,\mu\text{m}^2$, $M_x = M_z = 80$.

Hole defect in a slab waveguide

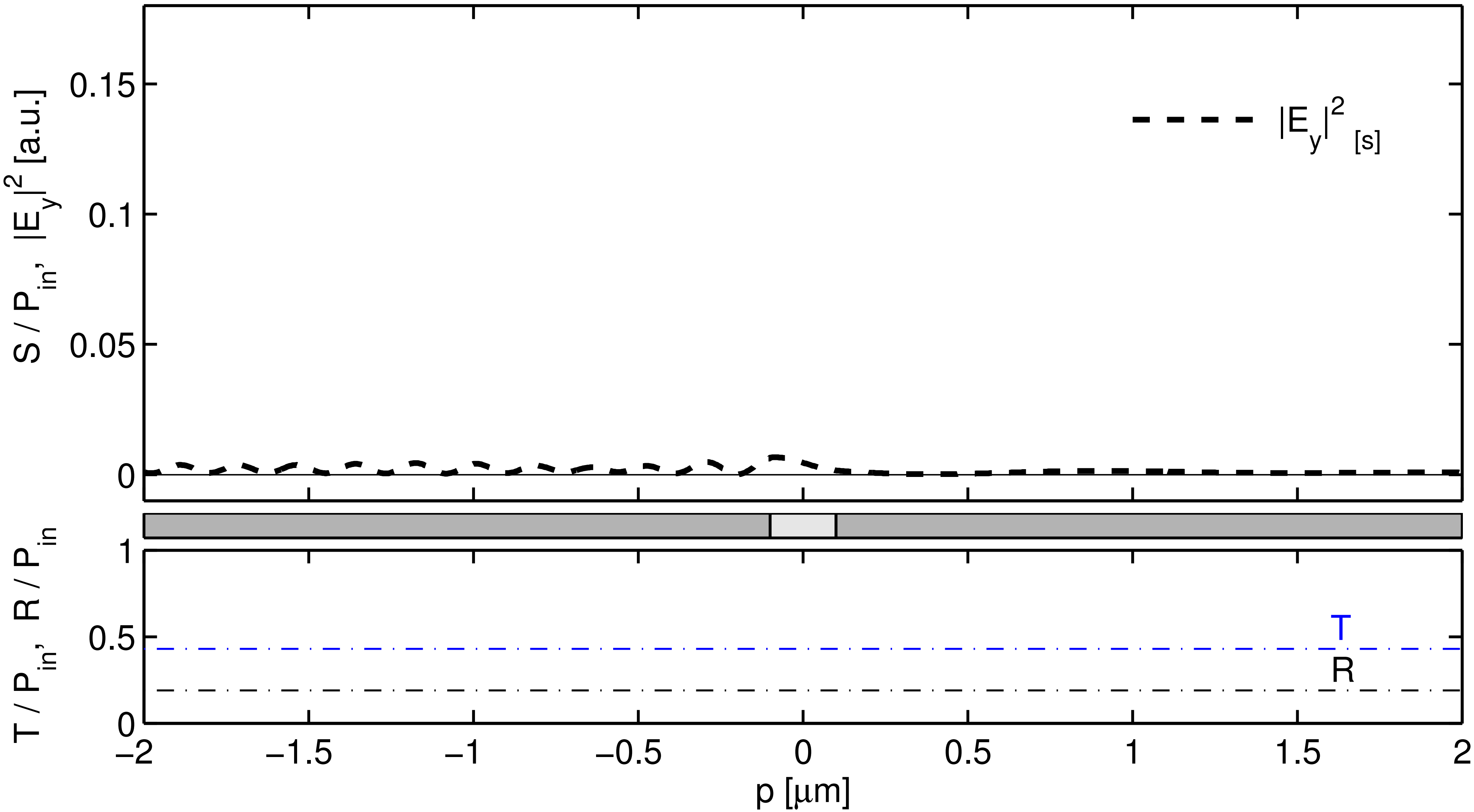

Hole defect in a slab waveguide

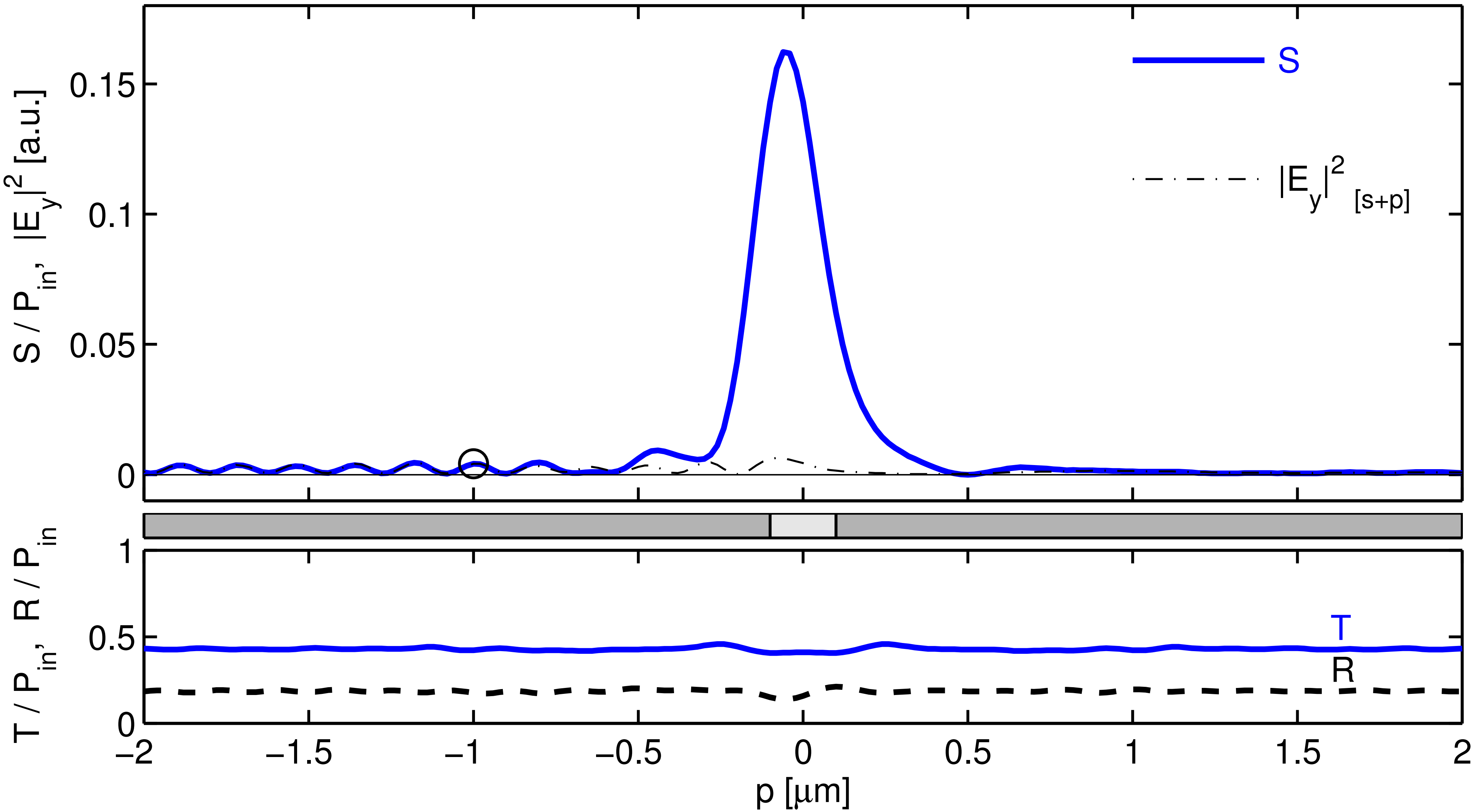

Hole defect in a slab waveguide

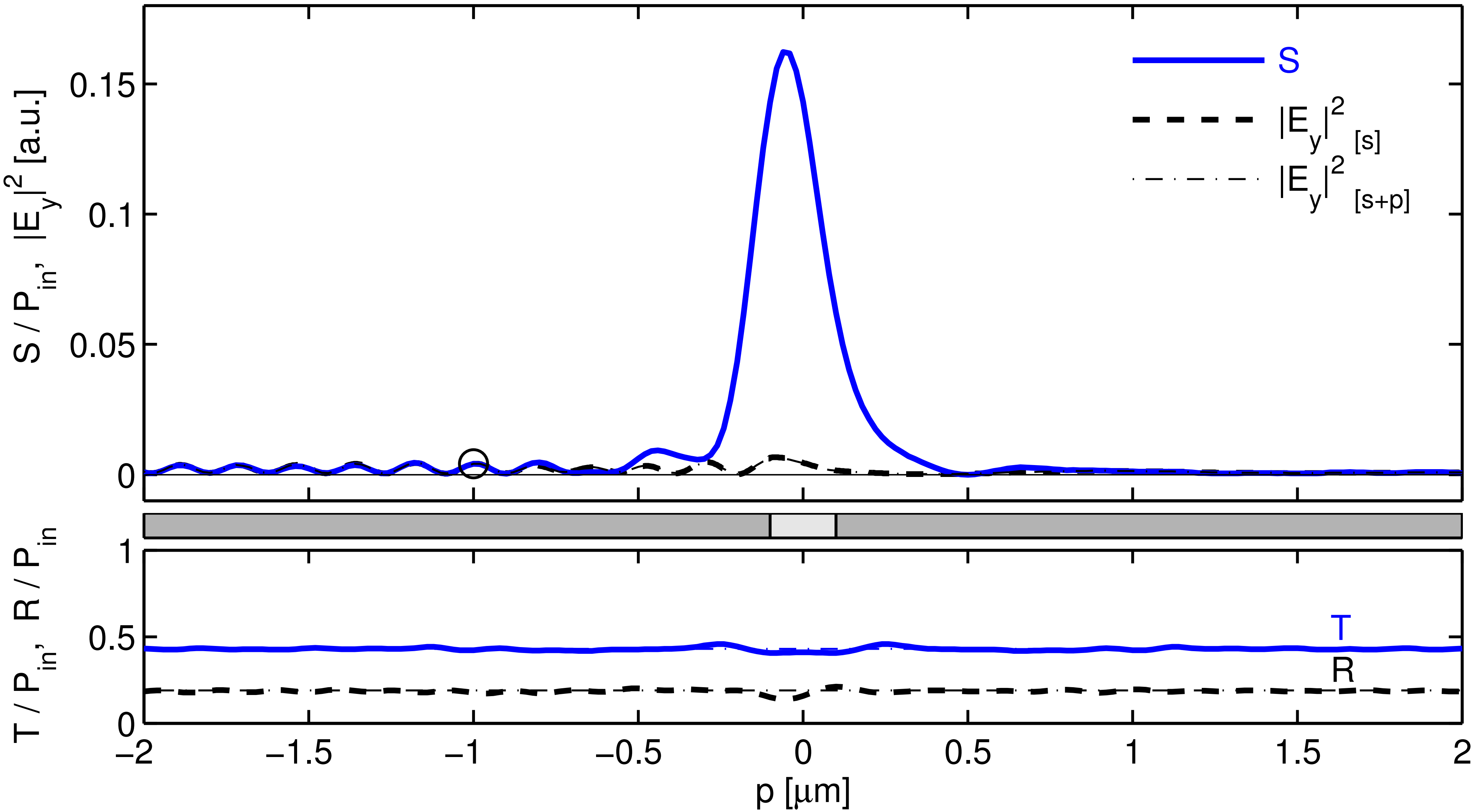

Short waveguide Bragg grating

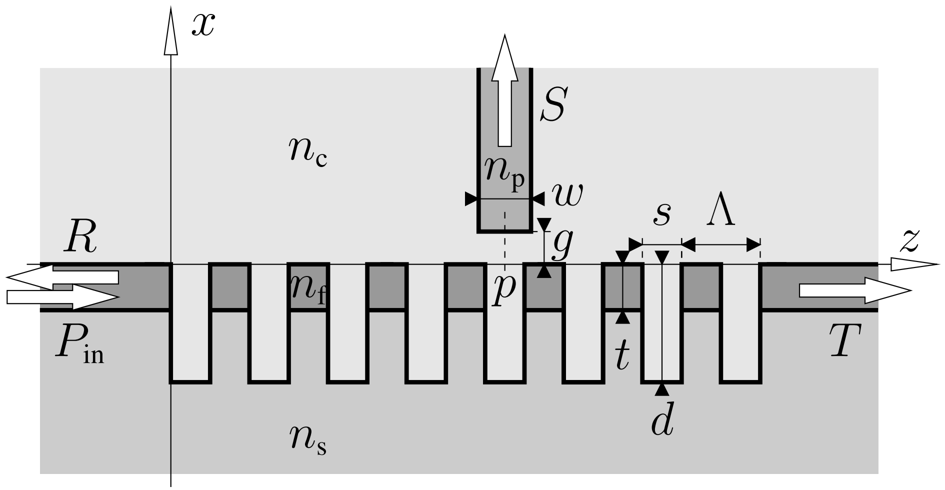

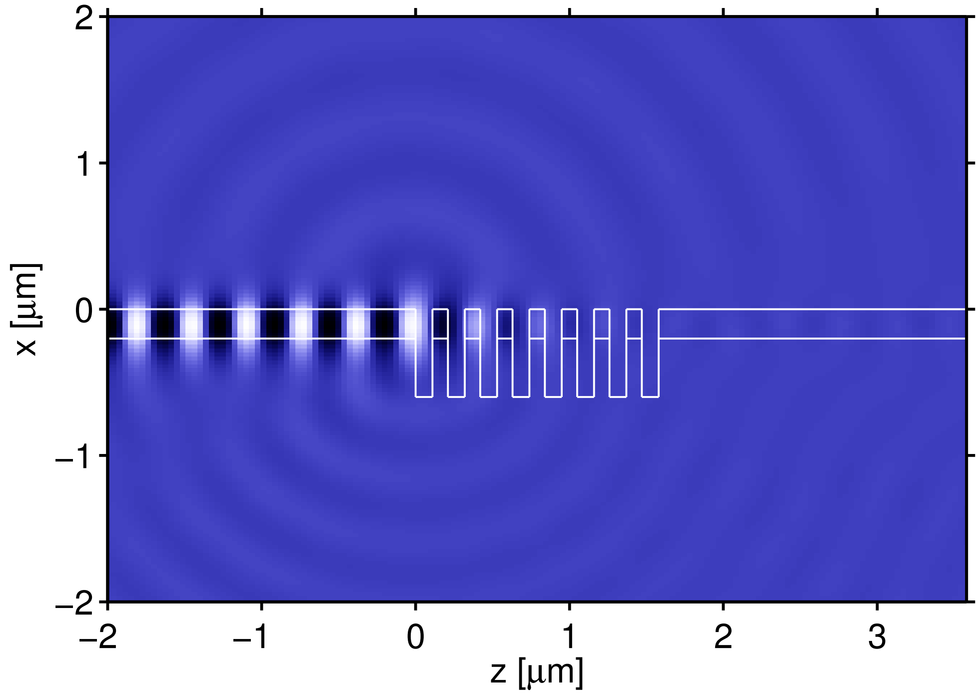

$n_s = 1.45$, $n_f = 2.0$, $n_c = 1.0$, $t = 0.2\,\mu$m, $d = 0.6\,\mu$m,
$\Lambda = 0.21\,\mu$m, $s = 0.11\,\mu$m, $g = 10\,$nm, $w = 100\,$nm, $n_p = 1.5$,
TE, $\lambda = 0.633\,\mu$m, $(x, z) \in [-3.0, 3.0] \times [-3.0, 4.58]\,\mu\text{m}^2$, $M_x = 100$, $M_z = 120$.

Short waveguide Bragg grating

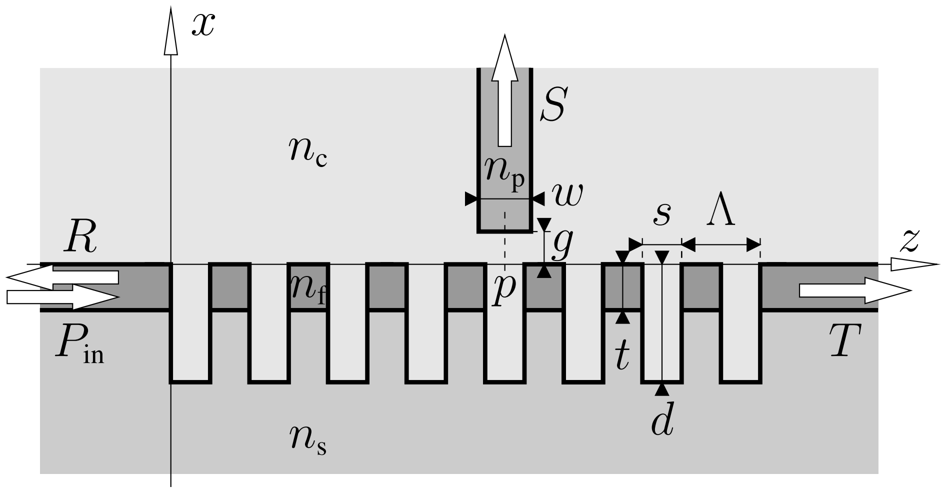

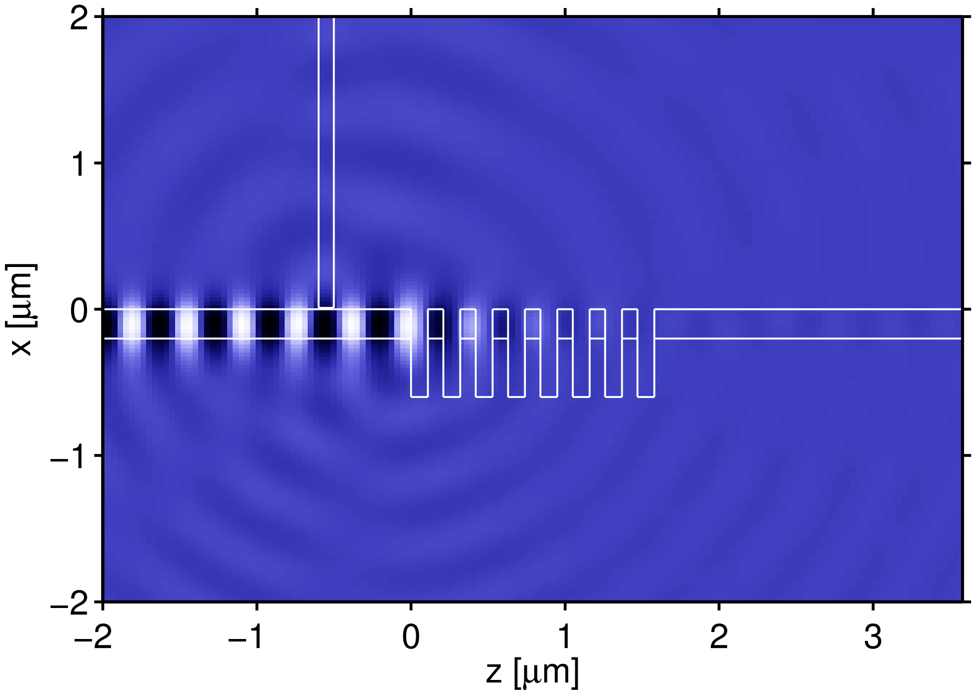

$n_s = 1.45$, $n_f = 2.0$, $n_c = 1.0$, $t = 0.2\,\mu$m, $d = 0.6\,\mu$m,
$\Lambda = 0.21\,\mu$m, $s = 0.11\,\mu$m, $g = 10\,$nm, $w = 100\,$nm, $n_p = 1.5$,
TE, $\lambda = 0.633\,\mu$m, $(x, z) \in [-3.0, 3.0] \times [-3.0, 4.58]\,\mu\text{m}^2$, $M_x = 100$, $M_z = 120$.

Short waveguide Bragg grating

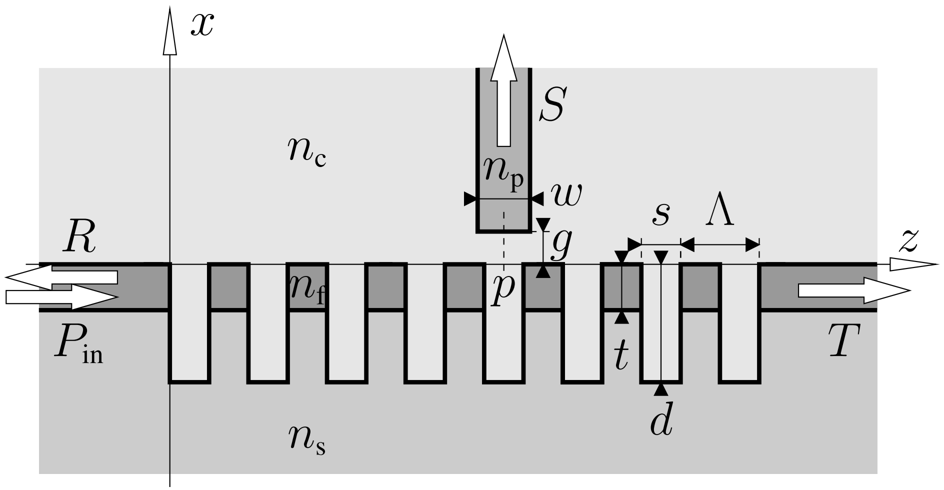

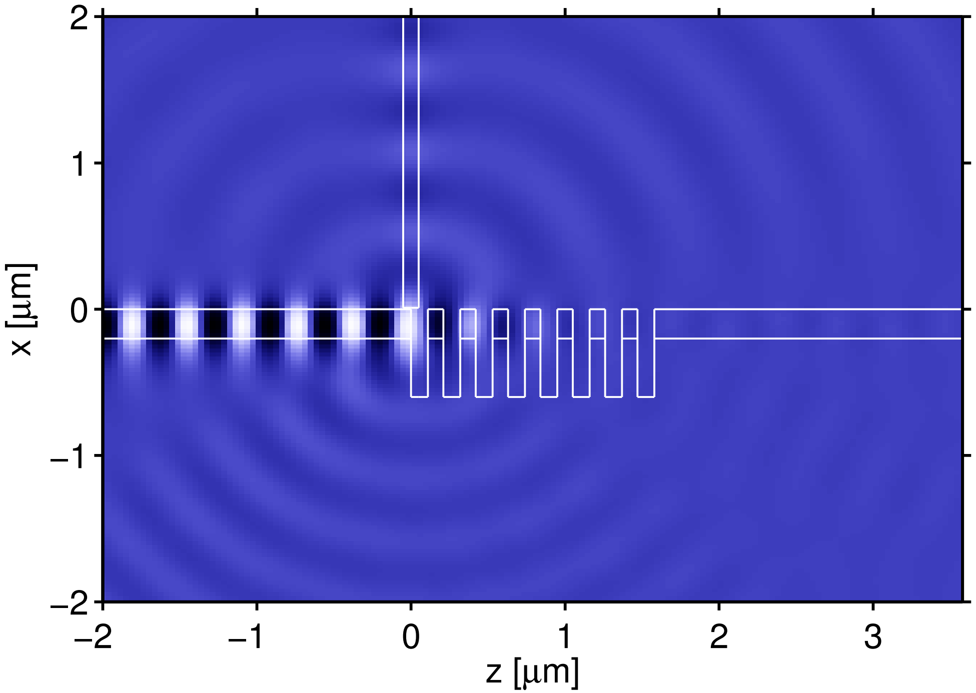

$n_s = 1.45$, $n_f = 2.0$, $n_c = 1.0$, $t = 0.2\,\mu$m, $d = 0.6\,\mu$m,
$\Lambda = 0.21\,\mu$m, $s = 0.11\,\mu$m, $g = 10\,$nm, $w = 100\,$nm, $n_p = 1.5$,
TE, $\lambda = 0.633\,\mu$m, $(x, z) \in [-3.0, 3.0] \times [-3.0, 4.58]\,\mu\text{m}^2$, $M_x = 100$, $M_z = 120$.

Short waveguide Bragg grating

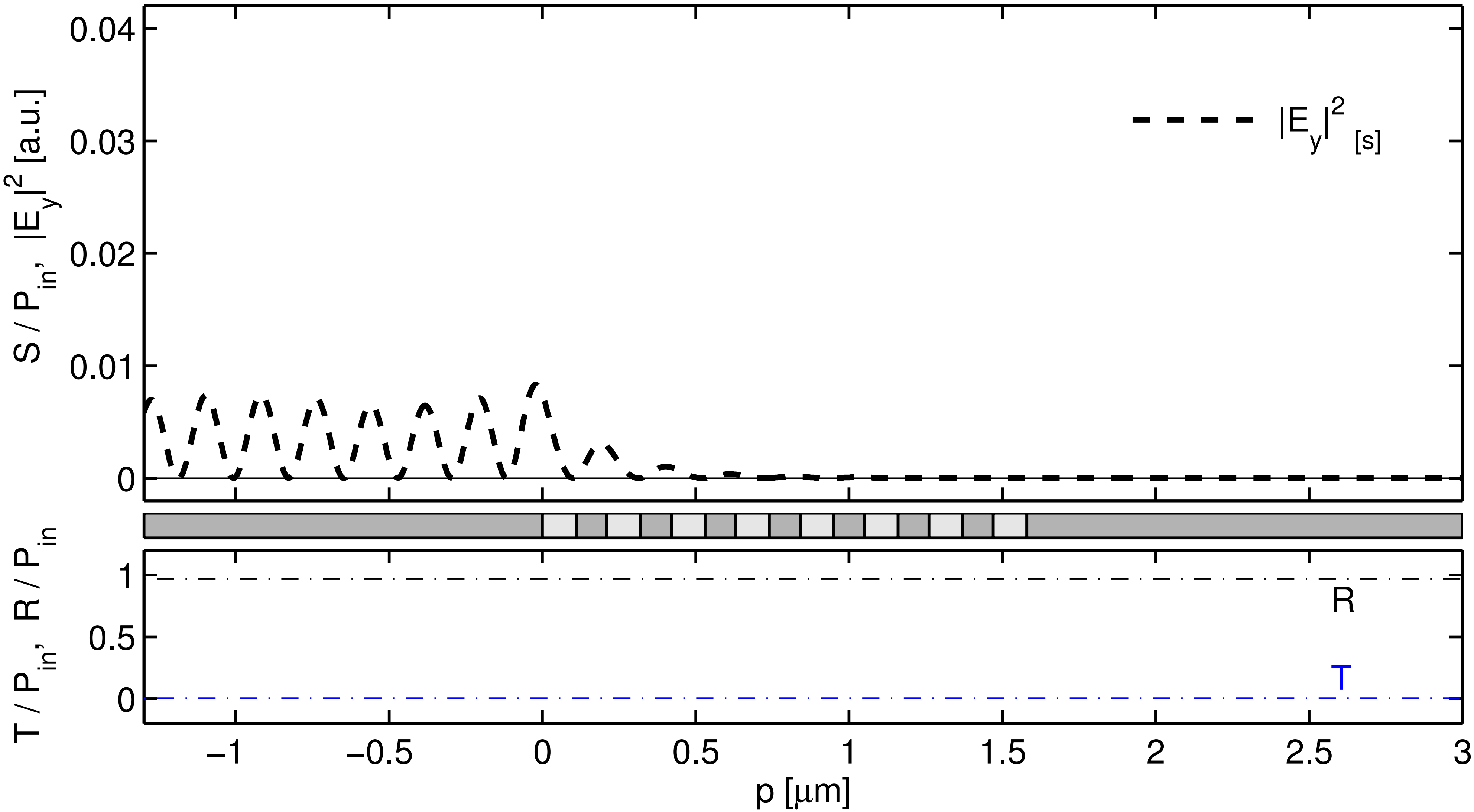

Short waveguide Bragg grating

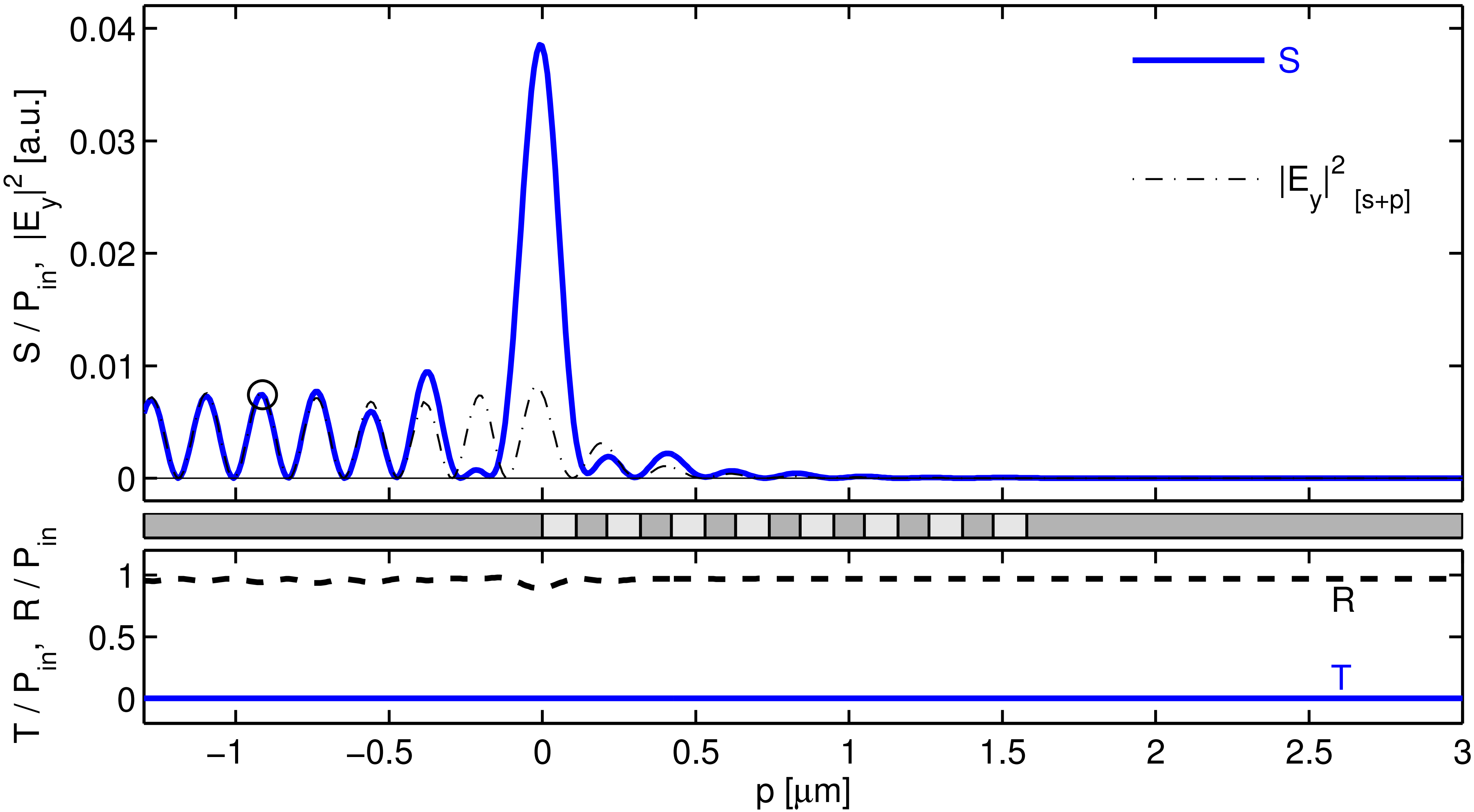

Short waveguide Bragg grating

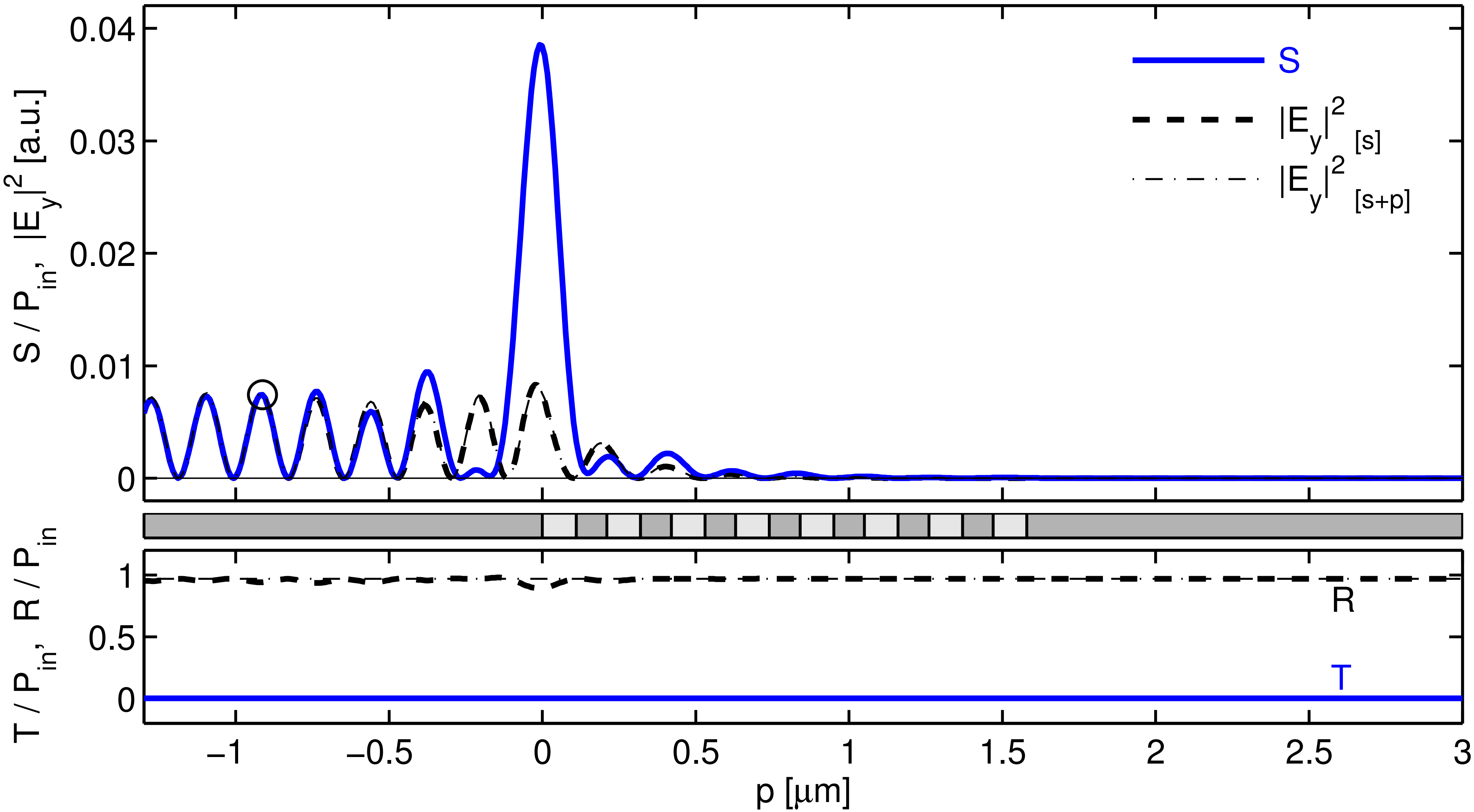

Resonant defect cavity

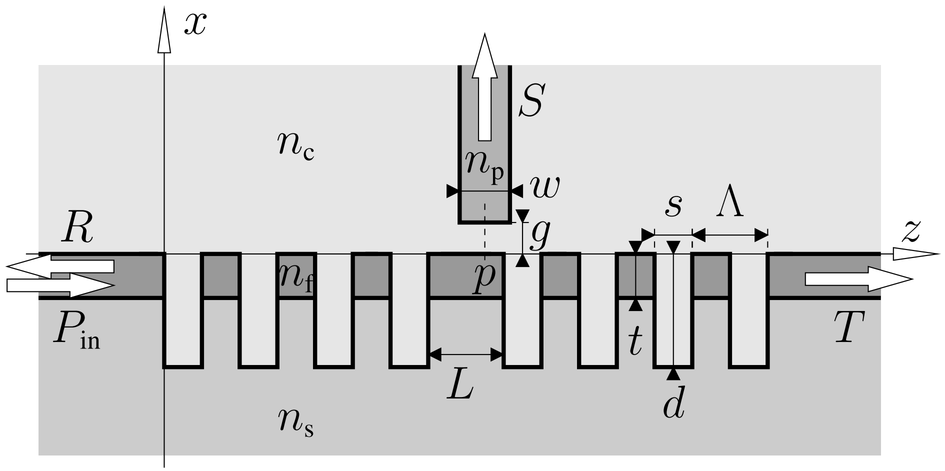

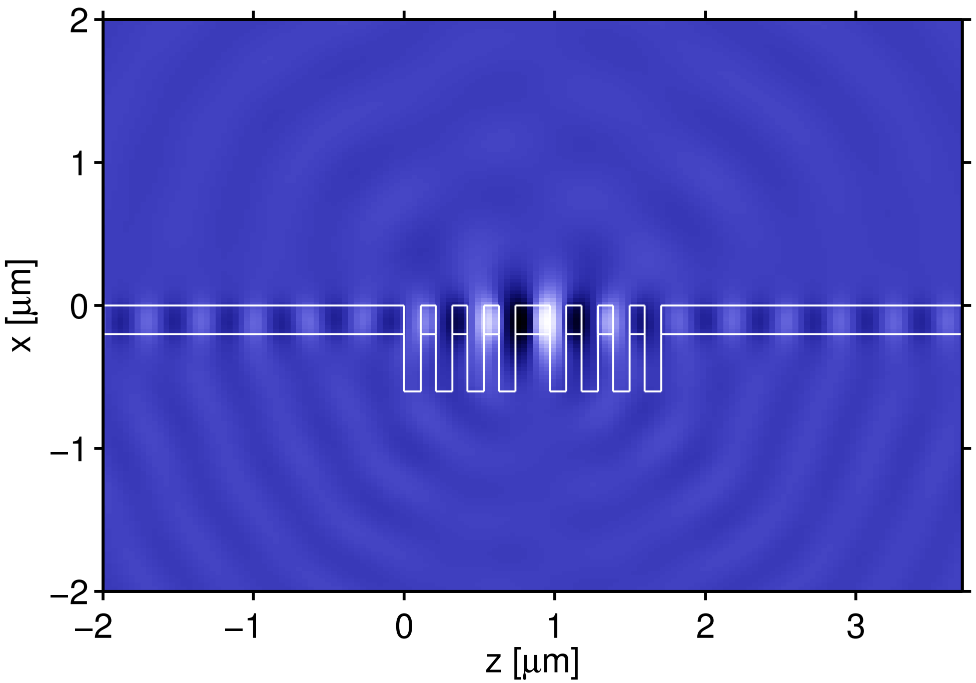

$n_s = 1.45$, $n_f = 2.0$, $n_c = 1.0$, $t = 0.2\,\mu$m, $d = 0.6\,\mu$m,
$\Lambda = 0.21\,\mu$m, $s = 0.11\,\mu$m, $L = 0.2275\,\mu$m, $g = 10\,$nm, $w = 100\,$nm, $n_p = 1.5$,
TE, $\lambda = 0.633\,\mu$m, $(x, z) \in [-3.0, 3.0] \times [-3.0, 4.7075]\,\mu\text{m}^2$, $M_x = 100$, $M_z = 120$.

Resonant defect cavity

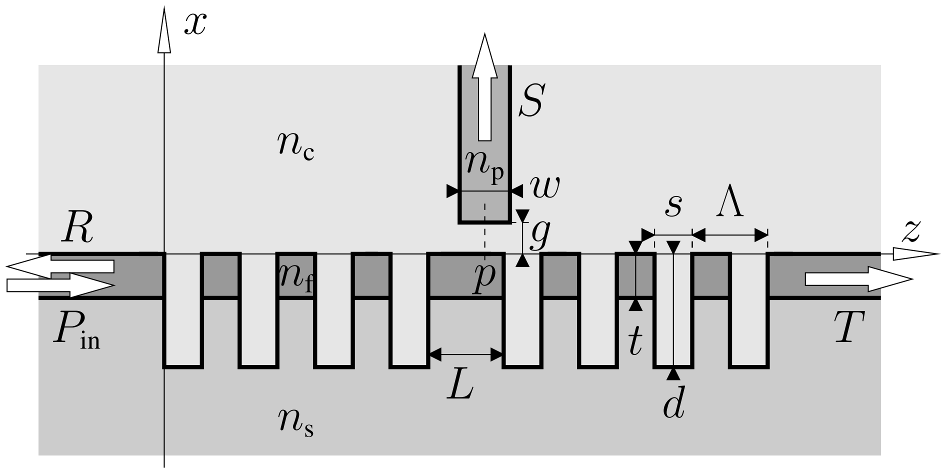

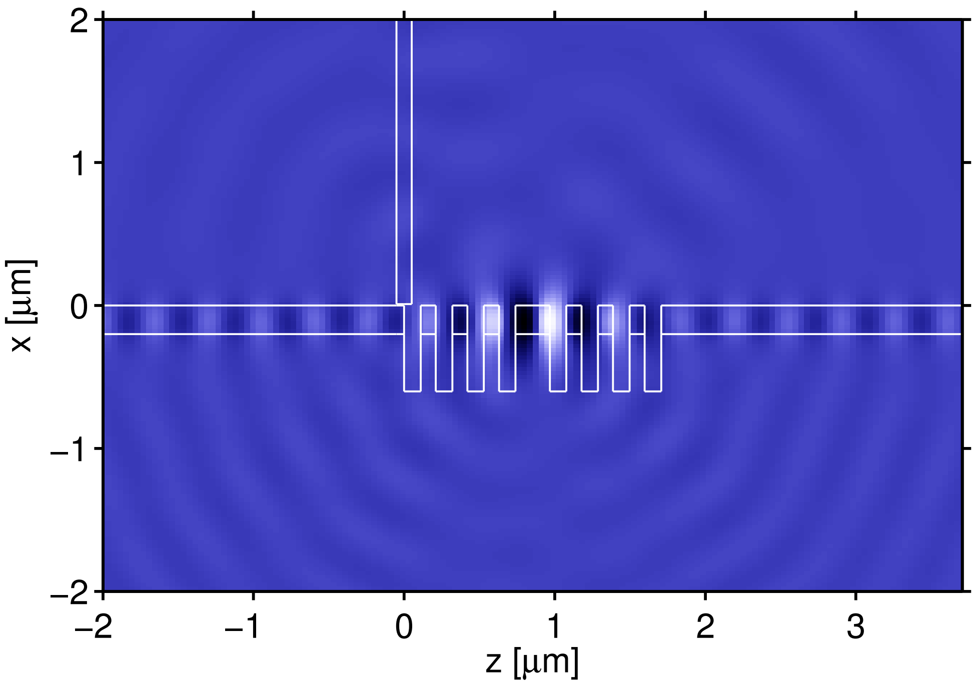

$n_s = 1.45$, $n_f = 2.0$, $n_c = 1.0$, $t = 0.2\,\mu$m, $d = 0.6\,\mu$m,
$\Lambda = 0.21\,\mu$m, $s = 0.11\,\mu$m, $L = 0.2275\,\mu$m, $g = 10\,$nm, $w = 100\,$nm, $n_p = 1.5$,
TE, $\lambda = 0.633\,\mu$m, $(x, z) \in [-3.0, 3.0] \times [-3.0, 4.7075]\,\mu\text{m}^2$, $M_x = 100$, $M_z = 120$.

Resonant defect cavity

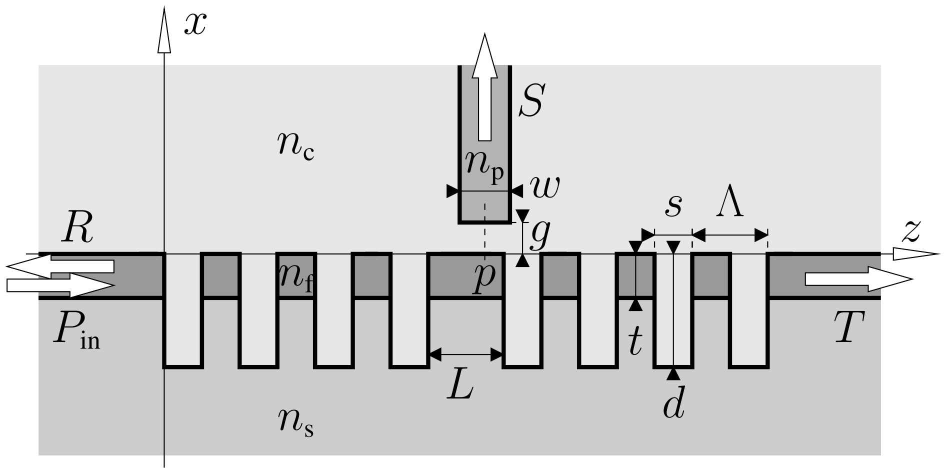

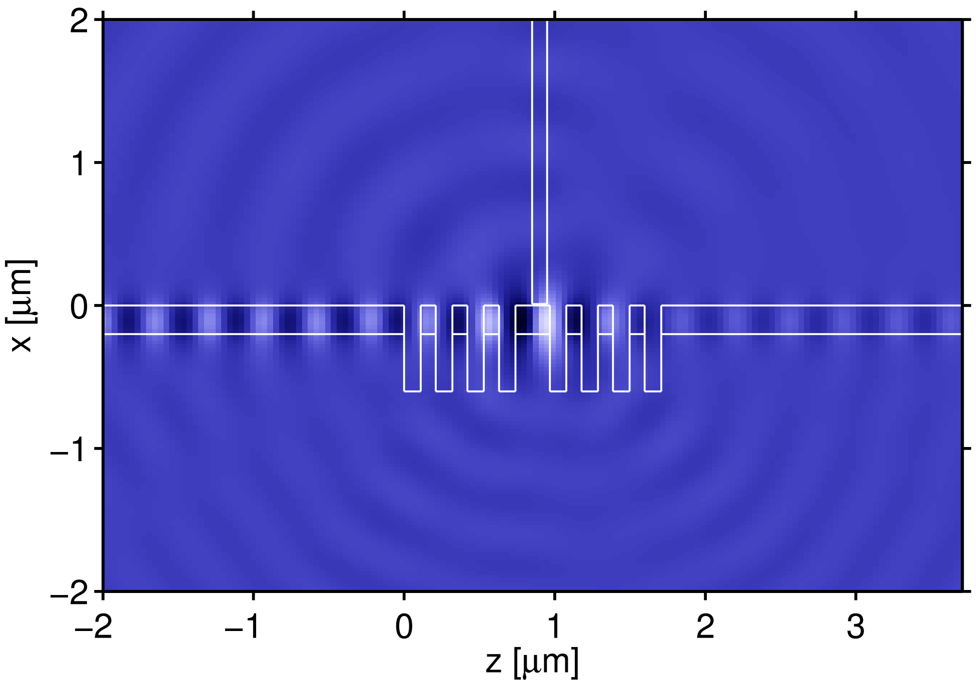

$n_\mathrm{s} = 1.45$, $n_\mathrm{f} = 2.0$, $n_\mathrm{c} = 1.0$, $t = 0.2\,\mu$m, $d = 0.6\,\mu$m,
$\Lambda = 0.21\,\mu$m, $s = 0.11\,\mu$m, $L = 0.2275\,\mu$m, $g = 10\,$nm, $w = 100\,$nm, $n_\mathrm{p} = 1.5$,
TE, $\lambda = 0.633\,\mu$m, $(x, z) \in [-3.0, 3.0] \times [-3.0, 4.7075]\,\mu\mathrm{m}^2$, $M_x = 100$, $M_z = 120$.

Resonant defect cavity

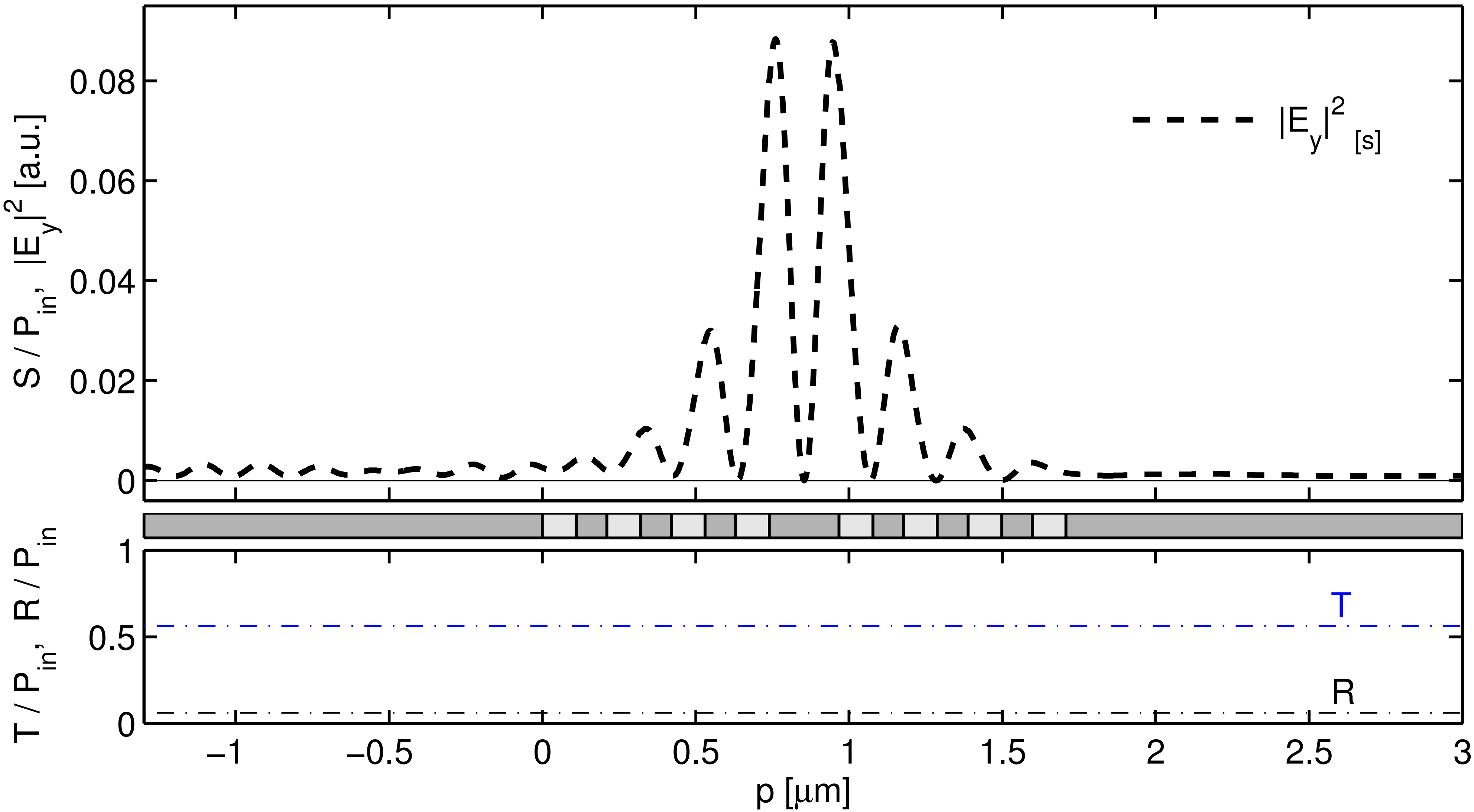

Resonant defect cavity

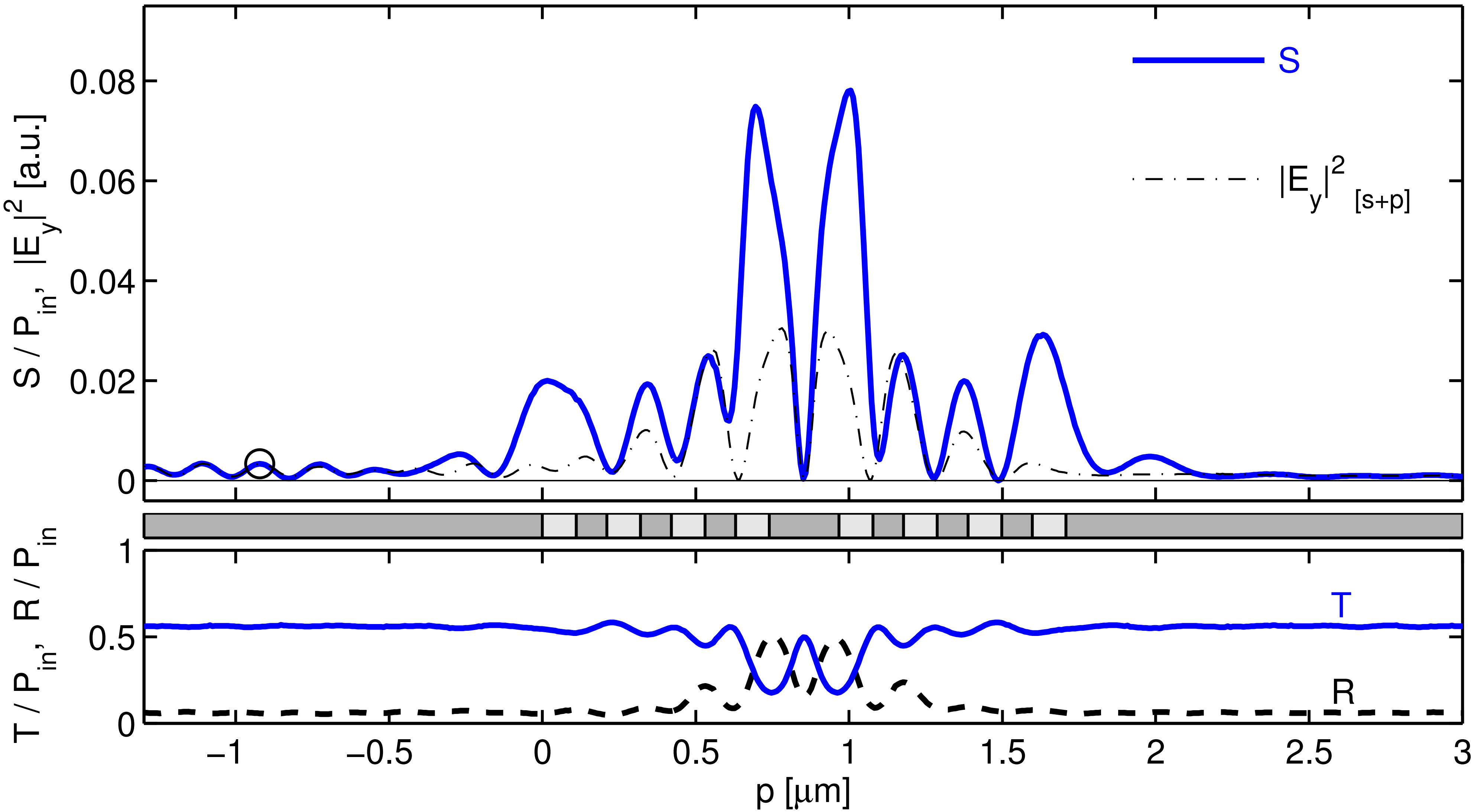

Resonant defect cavity

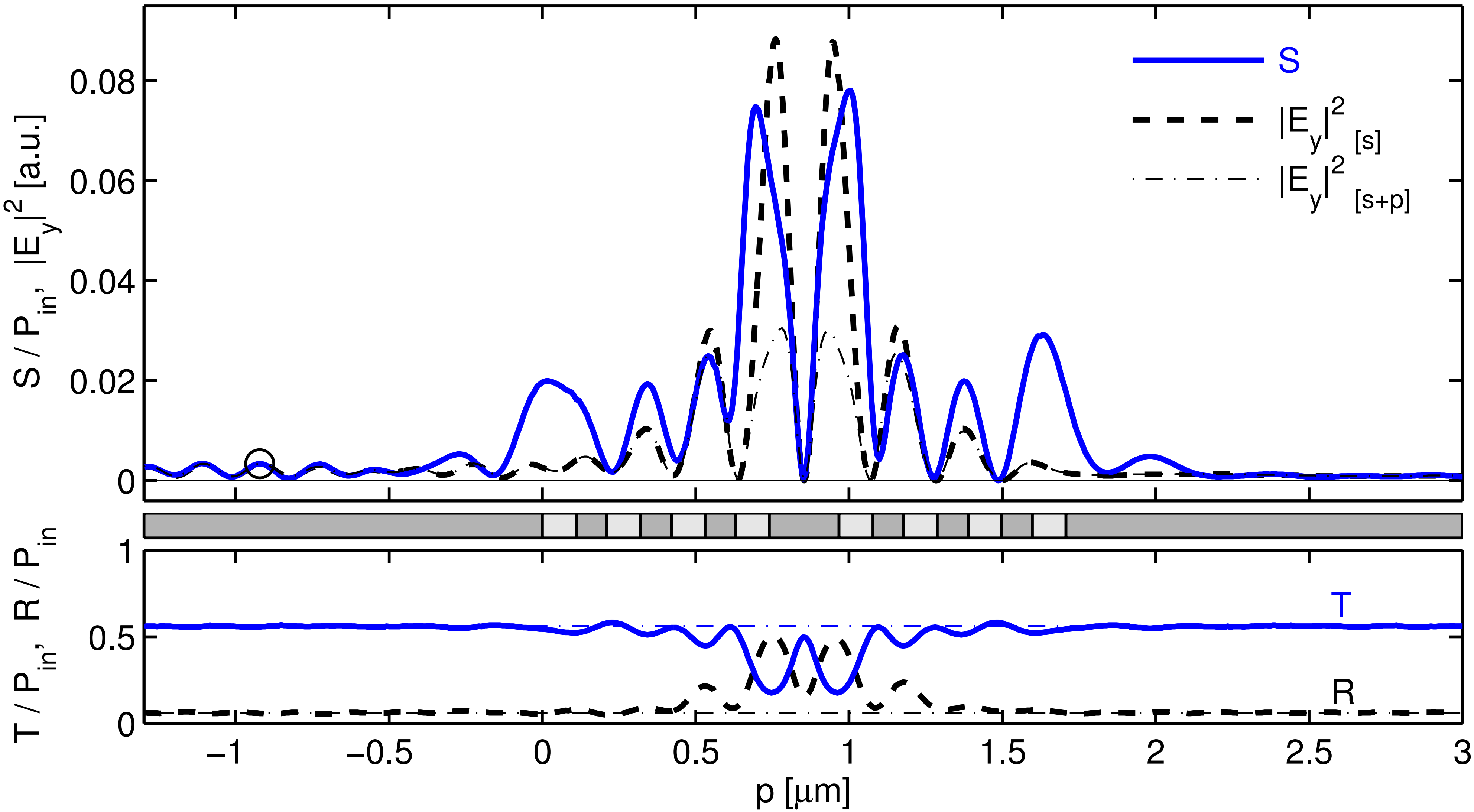

Bragg grating: PSTM experiment *

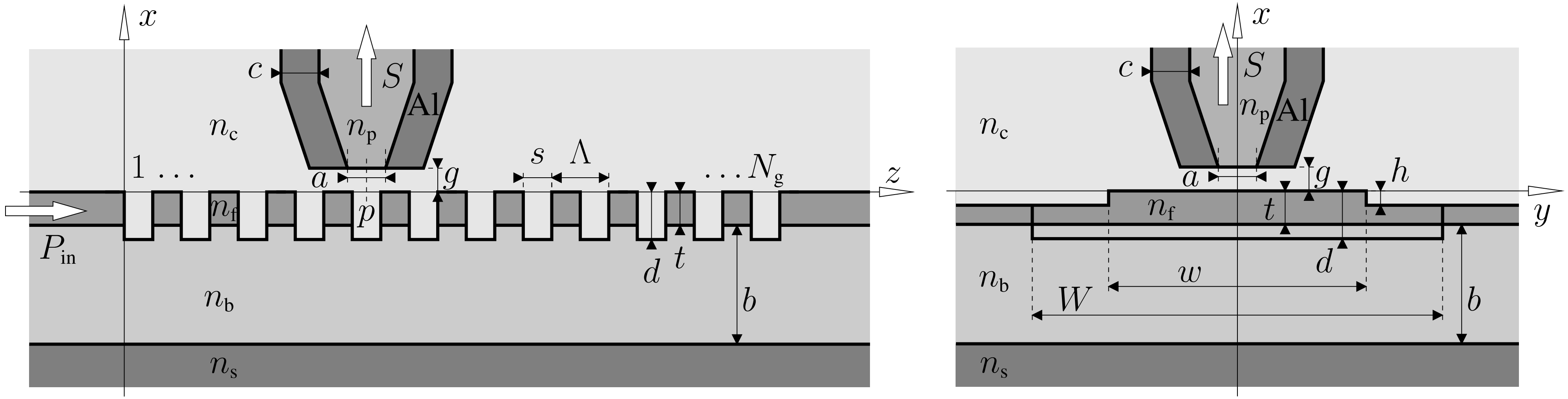

Sample: Rib waveguide with a series of deep, rectangular slits,
$n_s = 3.4$, $n_b = 1.45$, $n_f = 2.01$, $n_c = 1.0$, $t = 55\,$nm, $h = 11\,$nm, $w = 1.5\,\mu$m,
$W = 2.5\,\mu$m, $b = 3.2\,\mu$m, $\Lambda = 220\,$nm, $s = 110\,$nm, $d = 70\,$nm, $N_g = 15$.

Probe: Tapered cylindrical fiber tip with aluminium coating,
$a \approx 80\,$nm, $c \approx 100\,$nm, $g = 10\,$nm, $n_p = 1.5$;
TE polarized light, vacuum wavelength $\lambda = 0.6328\,\mu$m.

* E. Flück, M. Hammer, A. M. Otter, J. P. Korterijk, L. Kuipers, N. F. van Hulst,
Amplitude and phase evolution of optical fields inside periodic photonic structures,
Journal of Lightwave Technology **21**(5), 1384-1393 (2003)

Bragg grating: PSTM experiment

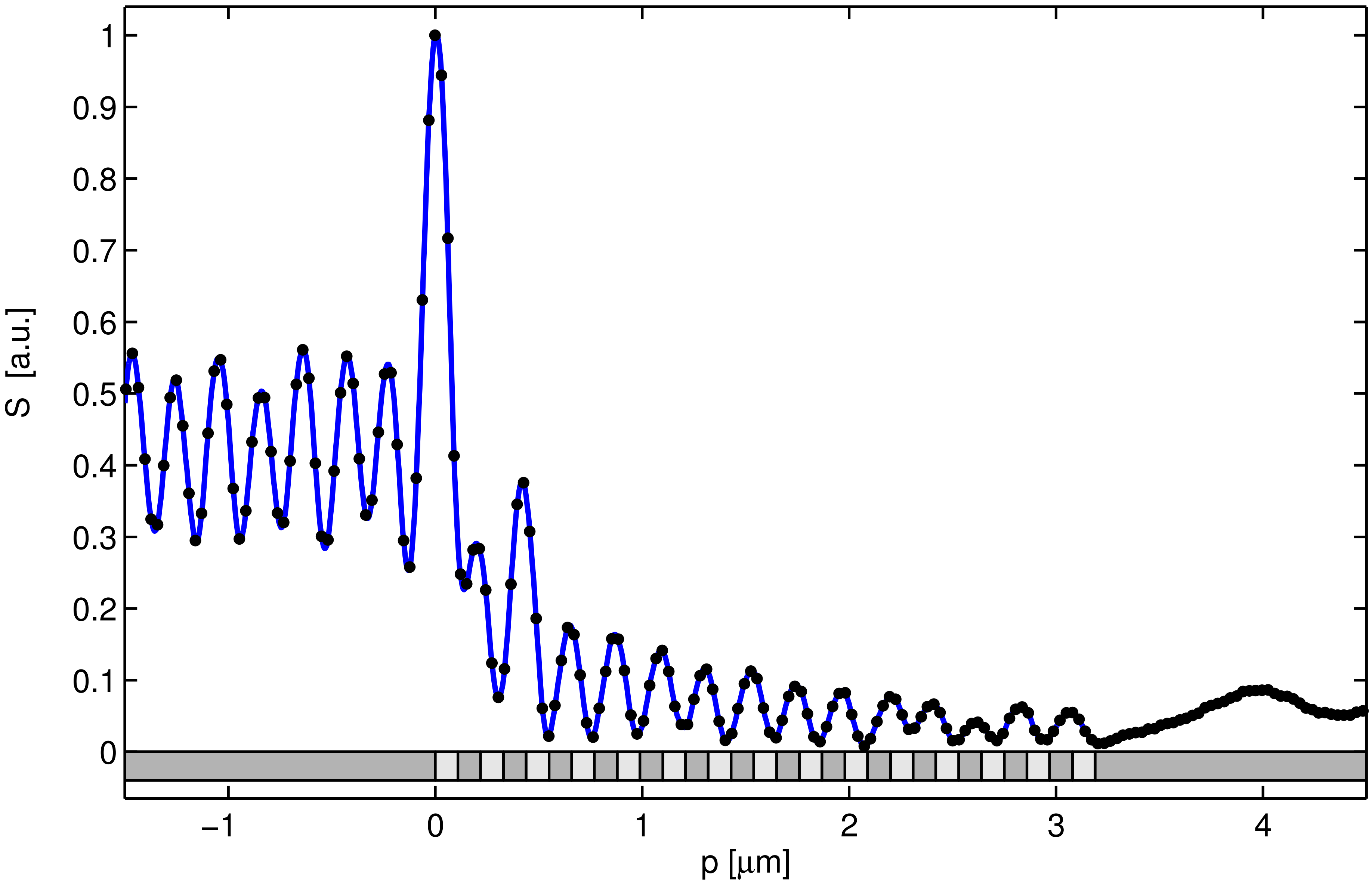

Bragg grating: QUEP model

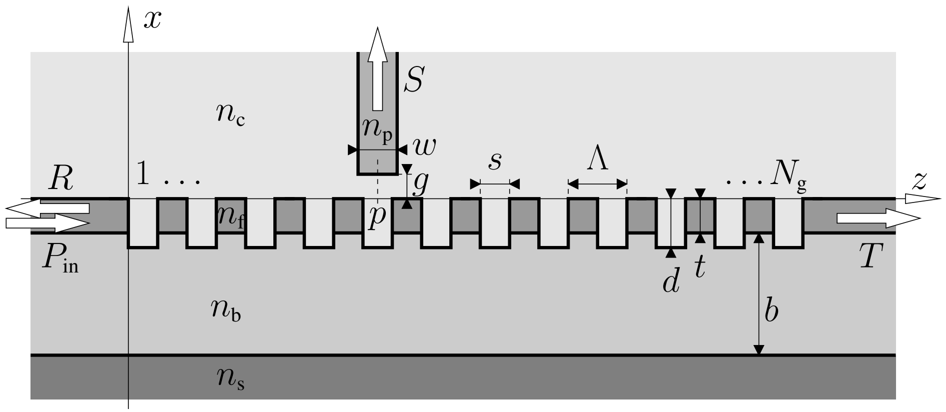

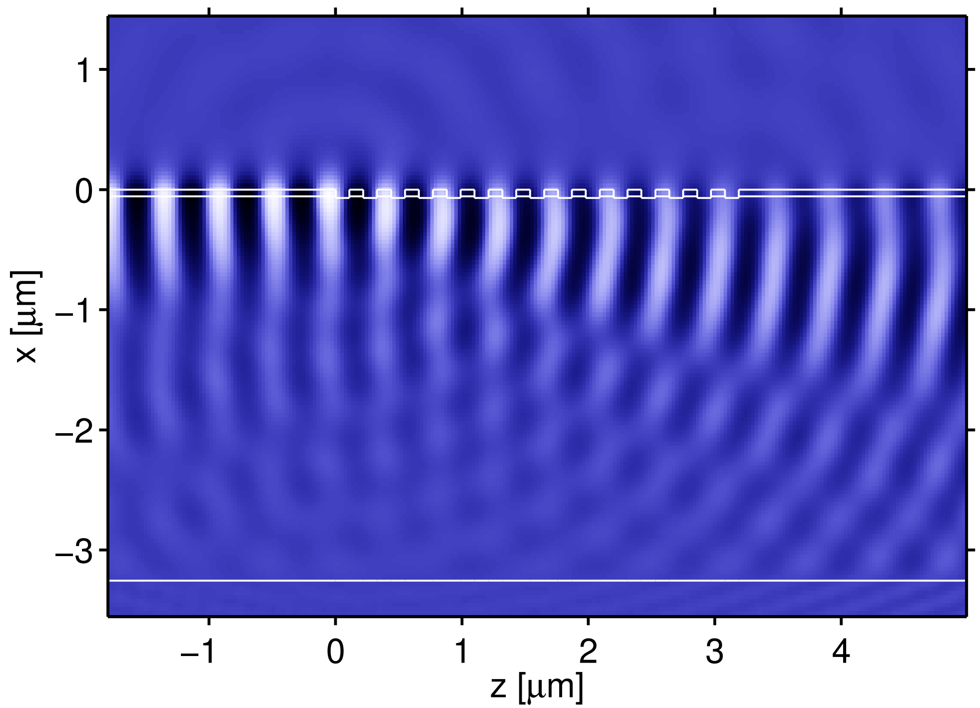

$n_s = 3.4$, $n_b = 1.45$, $n_f = 2.01$, $n_c = 1.0$, $t = 55\,\text{nm}$, $b = 3.2\,\mu\text{m}$, $d = 70\,\text{nm}$,
$\Lambda = 220\,\text{nm}$, $s = 110\,\text{nm}$, $N_g = 15$, $g = 10\,\text{nm}$, $w = 100\,\text{nm}$, $n_p = 1.5$,
TE, $\lambda = 0.6328\,\mu\text{m}$, $(x, z) \in [-3.5, 1.5] \times [-2.0, 5.2]\,\mu\text{m}^2$, $M_x = 80$, $M_z = 100$.

Bragg grating: QUEP model

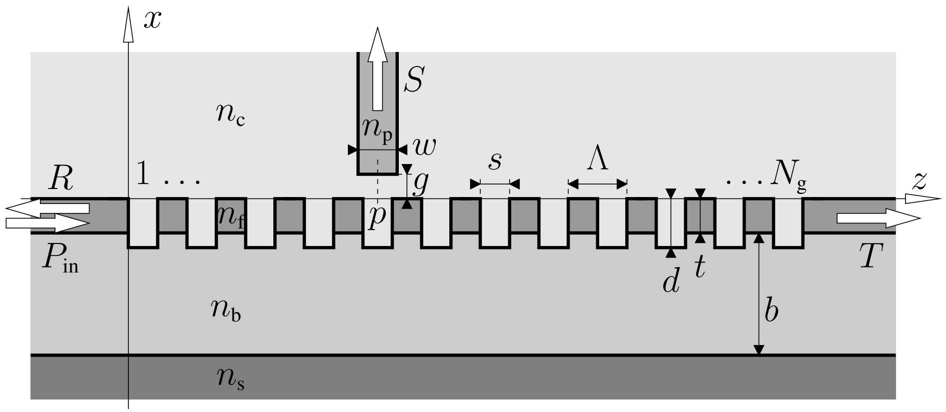

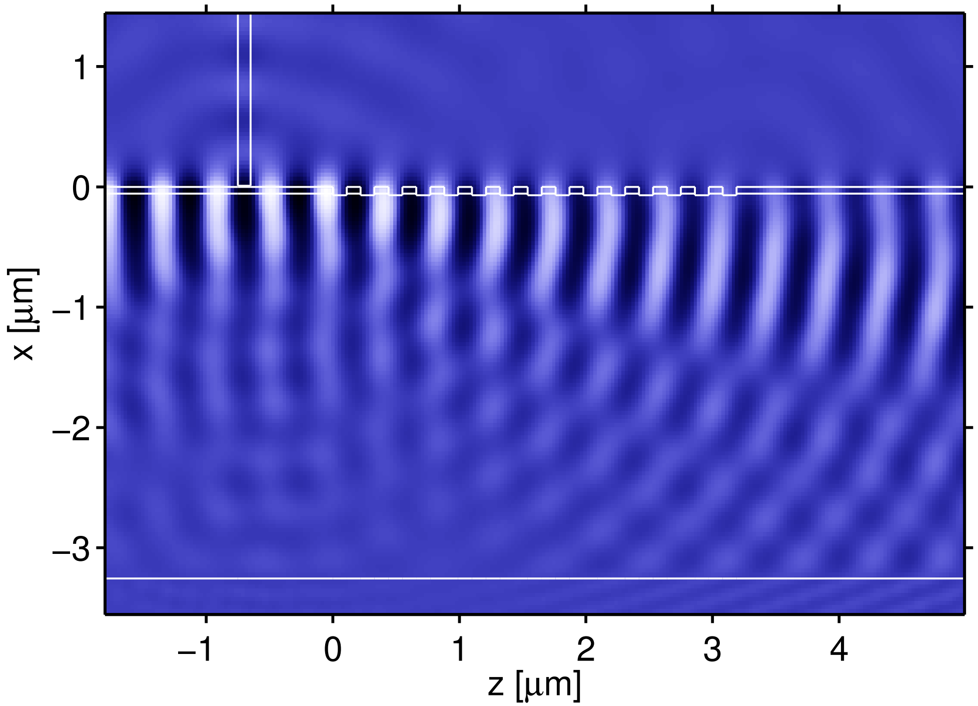

$n_\mathrm{s} = 3.4$, $n_\mathrm{b} = 1.45$, $n_\mathrm{f} = 2.01$, $n_\mathrm{c} = 1.0$, $t = 55\,\mathrm{nm}$, $b = 3.2\,\mu\mathrm{m}$, $d = 70\,\mathrm{nm}$,
$\Lambda = 220\,\mathrm{nm}$, $s = 110\,\mathrm{nm}$, $N_\mathrm{g} = 15$, $g = 10\,\mathrm{nm}$, $w = 100\,\mathrm{nm}$, $n_\mathrm{p} = 1.5$,
TE, $\lambda = 0.6328\,\mu\mathrm{m}$, $(x, z) \in [-3.5, 1.5] \times [-2.0, 5.2]\,\mu\mathrm{m}^2$, $M_x = 80$, $M_z = 100$.

Bragg grating: QUEP model

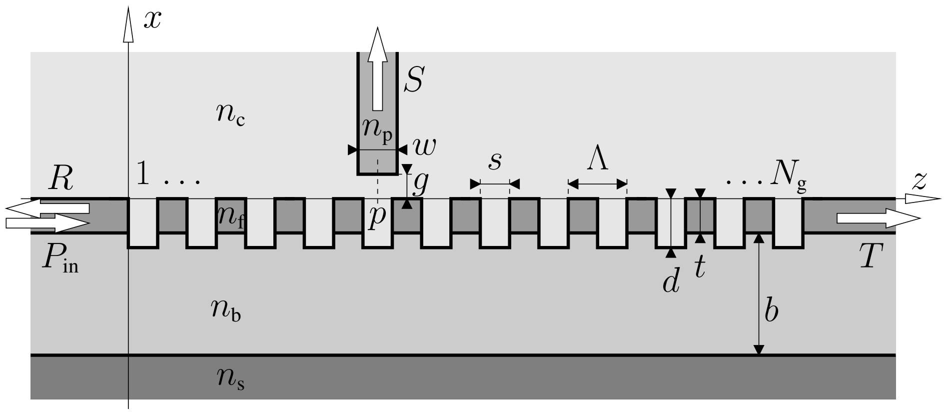

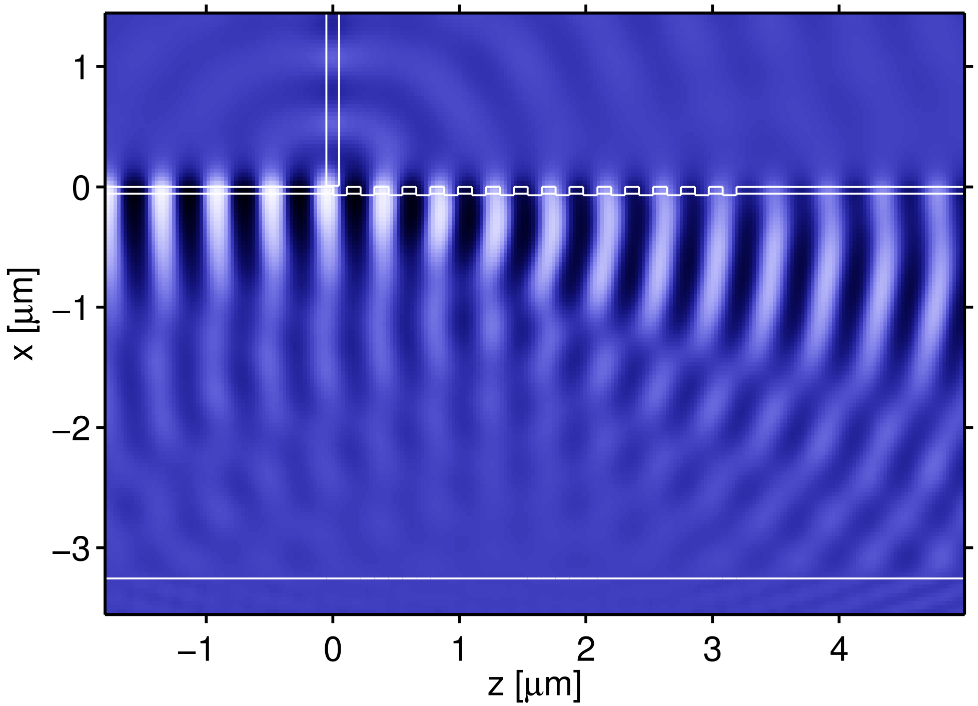

$n_s = 3.4$, $n_b = 1.45$, $n_f = 2.01$, $n_c = 1.0$, $t = 55\,$nm, $b = 3.2\,\mu$m, $d = 70\,$nm,
$\Lambda = 220\,$nm, $s = 110\,$nm, $N_g = 15$, $g = 10\,$nm, $w = 100\,$nm, $n_p = 1.5$,
TE, $\lambda = 0.6328\,\mu$m, $(x, z) \in [-3.5, 1.5] \times [-2.0, 5.2]\,\mu\text{m}^2$, $M_x = 80$, $M_z = 100$.

Bragg grating: QUEP model

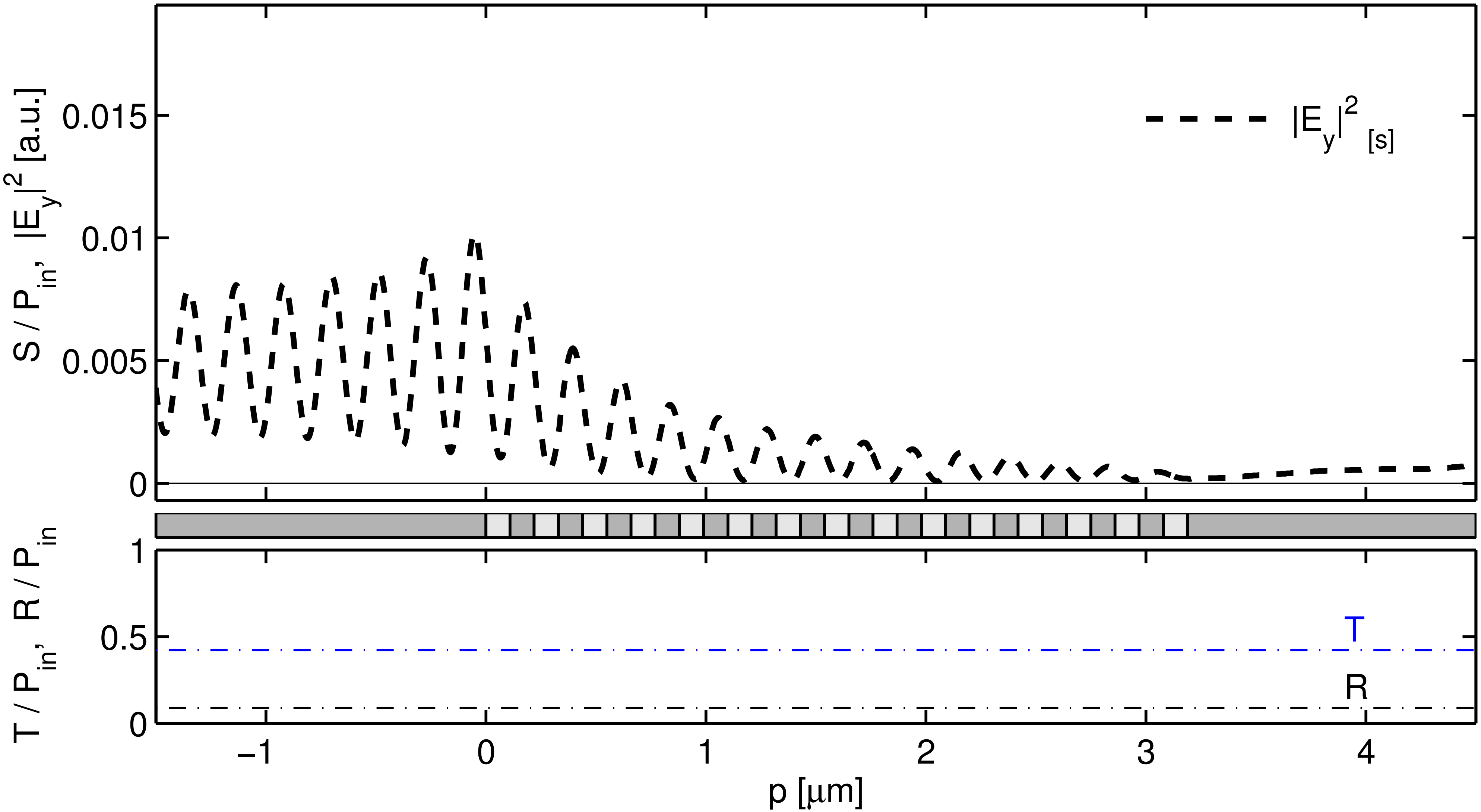

Bragg grating: QUEP model

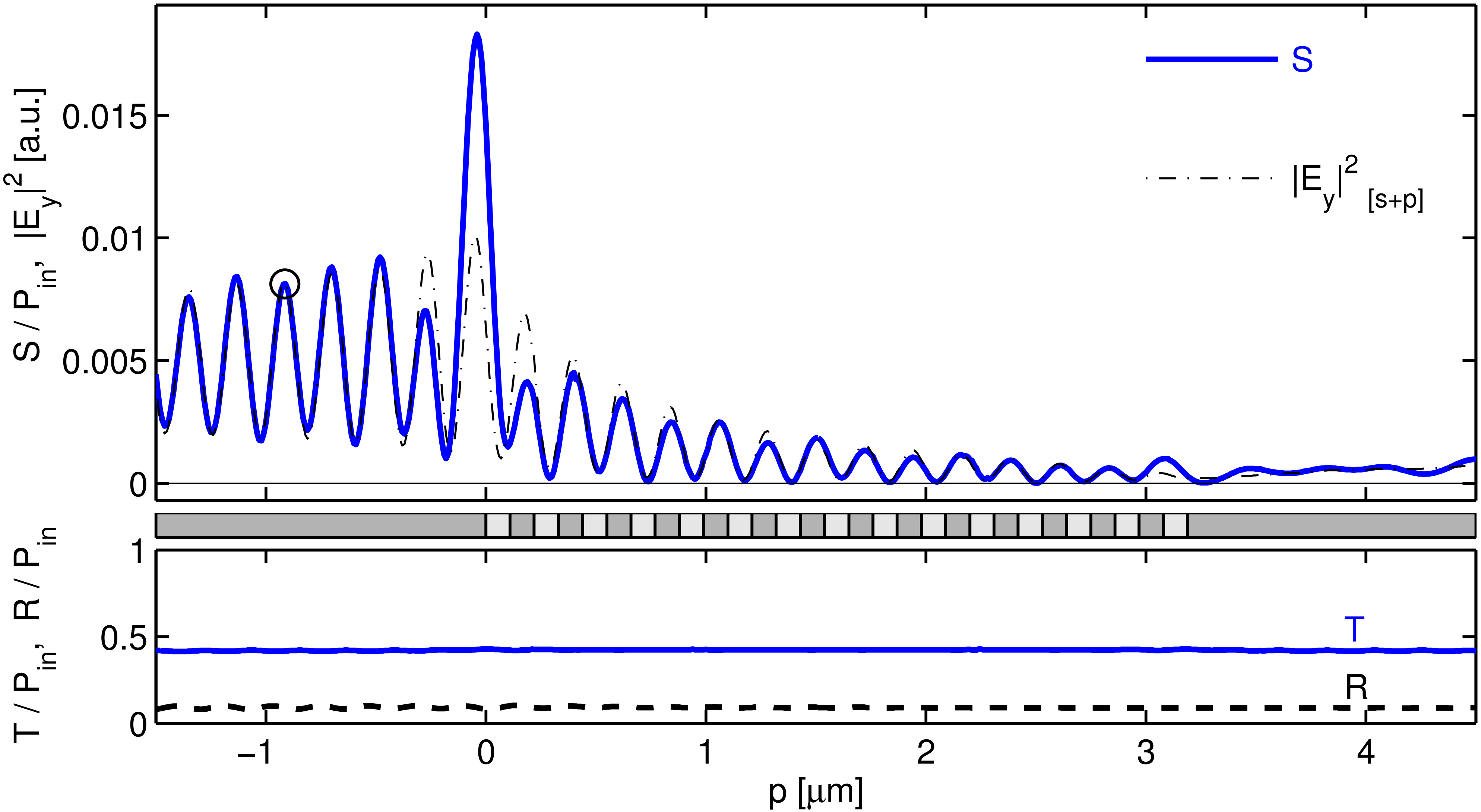

Bragg grating: QUEP model

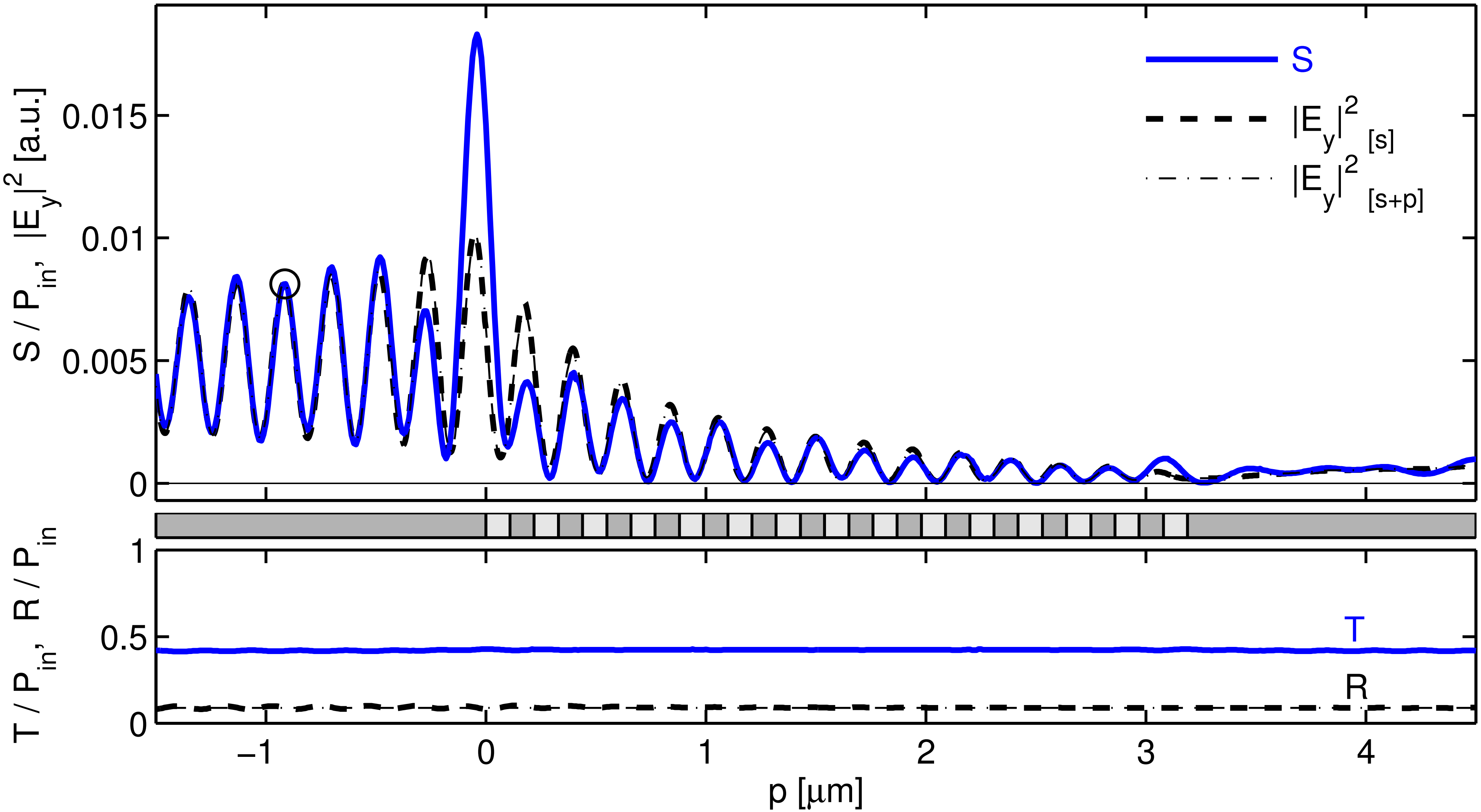

2-D PSTM modeling

QUEP scheme:

a semianalytical quadridirectional eigenmode expansion technique, here applied as convenient tool for "virtual" PSTM experiments:

- Evanescent field probing, signal $\not\sim |E|^2$.
- Direct scattering into the probe tip.
- Resonance breakdown caused by the presence of the probe.
- Reasonable mapping of evanescent fields for specific configurations.
- Ample qualitative agreement with real PSTM experiments on a waveguide Bragg grating.